TRIDHA
Journal of Clinical Cases & Reports
Volume 2023, Issue S16, 28 pages
https://doi.org/10.46619/joccr.2023.6.S16-1087

CLINICAL RESEARCH

Drug Innovation Studies Targeting Diabetes: A Computational Docking Approach on Multi-Drug Targets including COVID Inhibitors

Richa Goyal[1*], Manoj Kumar[2] and Anwar Mallick M[3]

[1]*Department of Biotechnology, Vinoba Bhave University, Hazaribagh, Jharkhand, India*
[2]*University Department of Zoology, VBU, Hazaribagh, India*
[3]*Botany Department and Department of Biotechnology, VBU, Hazaribagh, Jharkhand, India*

Correspondence should be addressed to Richa Goyal, PhD research scholar in department of Biotechnology, Vinoba Bhave University, Hazaribagh and Researcher in Department of Tech. Biosciences, Diginalix, Ranchi, Jharkhand, India

Received: 1 September 2023; Accepted: 18 September 2023; Published: 25 September 2023

ABSTRACT

BACKGROUND

At present, single-targeted antidiabetic drugs are unable to cure the disease. Diabetes mellitus cases are rising exponentially and promoting hyperglycemia with multifactorial disease conditions and also increasing susceptibility to microbial and viral infection (e.g.; Coronavirus). The study is concerned with *in-silico* analysis of the interaction and mechanism of action of bio-molecules on multiple targets of glucose metabolism to control hyperglycemia.

METHODS

In the present study, lead was prepared from *C. roseus* alkaloids ligand library (21 compounds) and then tested its molecular interaction with 4 drug targets (AMPK, DPP4, alpha-glucosidase and PPARγ) for antihyperglycemic effect. *In-silico* testing of lead compound vindoline (CID: 425978) with the targets was by advanced computational docking studies and system biology approaches.

RESULT

Molecular docking and MD simulation studies of vindoline with multiple targets show strong non-covalent interactions between them. Docking results of 5'-AMP-activated protein kinase (AMPK) activator metformin with AMPK1 and AMPK2 targets were -4.0 kcal/mol and -4.2 kcal/mol, while vindoline docked scores showed -6.2 and -6.3 kcal/mol respectively; Dipeptidyl peptidase 4 (DPP4) inhibitor vildagliptin with DPP4 target was -6.7 kcal/mol and for the vindoline -6.8 kcal/mol. Alpha-glucosidase inhibitor acarbose with the target was -6.7 kcal/mol, vindoline -6.8 kcal/mol and Peroxisome proliferator-activated receptor gamma (PPARγ) activator

pioglitazone with PPARγ nuclear receptor was -6.4 kcal/mol, while vindoline -6.1 kcal/mol. MD simulation results also support the good binding interaction of docking outcomes. Drulito and Osiris explorer's result shows that the bioactive compounds had good solubility (LogS = -3.12 mol/lit), absorption (CLogP = 1.32), permeation (Molecular weight = 456), action (TPSA = 88.54), drug likeness = +3.95, drug-score = 0.74, non-toxic characteristics.

CONCLUSION

C. roseus alkaloid vindoline (CID: 425978) has the potential to reduce blood glucose levels efficiently. Hence, it has a high probability of becoming a potent antihyperglycemic drug which will be further validated by wet lab and clinical trials.

KEYWORDS

Diabetes; AMPK; DPP4; Alpha glucosidase; PPARγ receptor; *C. roseus* alkaloids

ABBEVIATIONS

AMPK: AMP-Activated Protein Kinase

DPP4: Dipeptidyl Peptidase-4

$PPAR_{\gamma}$: Peroxisome Proliferator-Activated Receptor Gamma

GLUT4: Glucose transporter 4

UNL: Ligand

LEU: Leucine

GLU: Glutamic acid

PHE: Phenylalanine

ALA: Alanine

ARG: Arginine

GLY: Glycine

GLN: Glutamine

TYR: Tyrosine

ASP: Aspartic Acid

HIS: Histidine

THR: Threonine

LYS: Lysine

TYR: Tyrosine

ASN: Asparagine

SER: Serine

GLY: Glycine

TRP: Tryptophan

ASP: Aspartic acid

VAL: Valine

MET: Methionine

PRO: Proline

INTRODUCTION

The present *in-silico* research work is trying to find out certain natural compounds and clues of structure that can act on multiple targets of glucose metabolism. This will be further validated by wet lab and clinical tests. Diabetes mellitus cases are increasing exponentially and doubling every decade from a predictable 30 million cases in 1985 [1] to 463 million in 2019 and may become 700 million by 2045 [2]. Also, the International Diabetes Federation (IDF) atlas 2019 reported that India had 88 million diabetic cases, whereas in Jharkhand (a state in India), the cases were about 1 million [3]. About 1.2 million deaths occur per year due to diabetes in South East Asia, which is the 2nd highest death in the IDF region. At present, diabetes is the 9th major cause of death. The 2nd largest case of the disease has been reported in India. In 2013, international expenses on diabetes were approximately $548 billion or 11% of international expenditures on health [1], whereas in 2019 it was about 12% [4,5].

Diabetes mellitus is widely classified into 2 groups - Type I diabetes or insulin-dependent diabetes mellitus (IDDM), which is initiated by the absence of insulin secretion and Type II diabetes or non-insulin-dependent diabetes mellitus (NIDDM), which is primarily triggered by insulin resistance /insensitivity of target tissues to the insulin hormone. Type II diabetes is more recurrent than type I and about 90% to 95 % of cases of diabetes mellitus are related to type II diabetes [2,6]. This impaired condition in carbohydrate metabolism and absence of well-organized uptake and consumption of glucose by most cells of the body are causing secondary pathophysiological changes in multiple organ systems and promoting multifactorial disease conditions like abdominal obesity, fasting hyperglycemia, amplified blood triglycerides, reduced high - density lipoprotein - cholesterol, hypertension, glycosuria and tissue injury [1,7].

For the treatment of type II diabetes, several approaches; including oral drug remedies are taken care of which improve blood glucose control, reduce the toxic effect of glucose on beta cells, and increase endogenous insulin secretion. To fulfil the treatment aspect, many drug targets like AMPK, DPP4, Alpha-glucosidase, PPARγ etc are identified which help to maintain the normal blood glucose level and lifestyle of the patient [8,9] as shown in Figure 1.

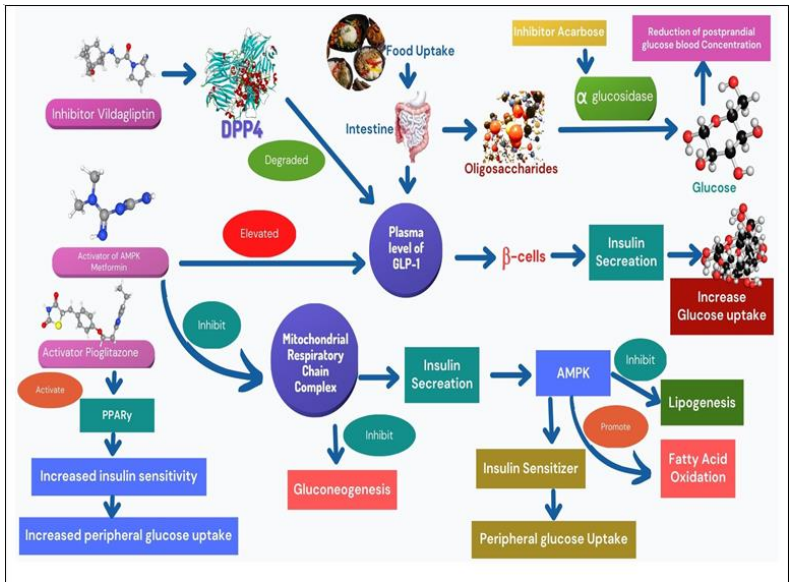

Figure 1: Representing different antidiabetic drug targets (AMPK, DPP4, α-glucosidase, PPARy) and mechanism of action of standard antihyperglycemic drug.

AMP-activated protein kinase (AMPK) is a cellular energy-sensing protein kinase that controls energy metabolism. Activator of AMPK enzyme plays a crucial role in the suppression of hepatic gluconeogenesis and enhances insulin-induced glucose intake in skeletal muscle. Accumulation of glucose in skeletal muscle decreases the breakdown of lipids in adipose tissue and improves fatty acid oxidation [8,10]. Metformin (N, N-dimethylbiguanide) is an AMPK activator and is used as a first-line drug for initial control of type 2 diabetes [11,12]. But it has side effects too, like delayed absorption of glucose, other hexoses, amino acids and Vit B12 in the small intestine, metallic taste, pain in the abdomen, nausea, anorexia, bloating, mild diarrhoea and fatigue-related problems [13].

Dipeptidyl Peptidase-4 (DPP4) enzyme is related to the rapid degradation of endogenous GLP-1, signal transduction, apoptosis, and immune regulation (positive regulator of T-cell co-activation) [14]. Also, it acts as a sensory receptor for coronavirus MERS-CoV2 in humans [10]. DPP4 inhibitors bind competitively and selectively with DPP4 and inhibit GLP-1 and GIP (incretin) degradation [15]. DPP-4 inhibitors are an alternative antidiabetic treatment [16] and can be recommended as 2nd line therapy after failure of a first-line drug (e.g.; metformin). Vildagliptin binds covalently in the DPP4 active site and inhibits it [15]. However, the drug is less selective because it also inhibits DPP8 and DPP9 and causes side effects like vomiting, loose stools, headache, rashes, sensitive reactions, edema and hepatotoxicity [8].

Alpha-glucosidase is a small intestine mucosal enzyme, crucial for catalyzing the final stage of carbohydrate digestion [5] and responsible for the conversion of oligosaccharide into monosaccharide and increases blood glucose level [4,14,17]. The competitive inhibition of alpha-glucosidase takes place by an inhibitor that competes with the oligosaccharides and also interferes in its cleavage into monosaccharides from the carbohydrate-binding region. In the late postprandial period, its inhibitor raises plasma GLP-1 and decreases GIP levels and plasma insulin [6]. The α-glucosidases inhibitors (Acarbose, miglitol, and voglibose) are used as a third-line antidiabetic drug [13]. Acarbose (complex oligosaccharide) reversibly inhibits α-glucosidases, declines postprandial hyperglycemia, and lowers HbA1c moderately (by 0.4%-0.8%). Regular use of Acarbose in the initial phase of the disease reduces the incidence of type 2 diabetes in addition to hypertension and cardiac disease but has side effects related to gastrointestinal problems like flatulence, intestinal discomfort and loose stool due to fermentation of unutilized carbohydrates [8] and hepatitis [18].

Peroxisome proliferator-activated receptor gamma (PPARγ) is a nuclear receptor. Its expression is mainly observed in fat tissues, but up to some extent in muscle and some other cells too. Its agonist pioglitazone promotes the RNA synthesis of several insulin-responsive genes [8], activates the genes that are involved in adipogenesis and lipid metabolism of adipose tissues [14], reverses insulin resistance and improves GLUT4 expression. It enhances glycemic control and, as a result, decreases HbA1C and insulin levels in diabetic patients [19]. Pioglitazone has some side effects like elevation in plasma volume, declination in haemoglobin and haematocrit, edema, weight gain and probability of hypoglycemia etc. [20].

With time, many new approaches have been explored to combat diabetes and its complications, but it is still a challenge for researchers and medical scientists to cure the disease [21-23]. As per literature natural compounds have a wide structural range of pharmacological actions and are used to treat a range of diseases and infections.

In the Ayurvedic literature, Sushruta Samhita and Charaka Samhita literature reported more than 500 species of antidiabetic plants [24,25] and in some literature, more than 1200 plant species are reported to have hypoglycaemic ability [21].

Catharanthus roseus (Vinca rosea) belongs to the *Apocynaceae* family and is commonly known as sada bahar/ periwinkle. It is well recognized for its action against tumours, microbes, and hyperglycemia. This plant is rich in alkaloids, flavonoids and phenolic compounds. The *C. roseus* alkaloids (Catharanthine, leurosinesulfate, lochnerine, vindoline, vindolinine and tetrahydroalstonine) can decrease blood sugar levels [26] and delay diabetes-induced cataract formation [27-32] but how it works is still unexplored.

The drug development process is a very expensive and time-consuming task [33,34]. In this study, we have selected a small perennial plant growing all around the world, *C. roseus* and tried to identify biomolecules and their structure having fewer or no side effects and act on multiple therapeutic target sites to adequately reduce blood glucose levels as well as effectively control secondary pathological aspects of diabetes too. By using advanced computational and docking approaches we predicted/identified certain natural compounds having antihyperglycemic potential, with a low/no toxic effect in contrast to synthetic drugs for the same doses. Further experimental validation will be required for becoming a successful drug candidate for diabetes.

METHODS

Selection of Drug Target

The structure of target proteins like AMPK (Uniprot ID- Q13131, P54646), DPP-4 (Uniprot ID- P27487), α-glucosidase (Uniprot ID- O43451), PPARγ (Uniprot ID-P37231) of human were identified and downloaded from Uniprot [10]. The PDB crystal structure of the protein is a specific condition crystal structure and does not constitute a representative subset of every protein [35]. Therefore, may not be able to represent all variations from normal to diseased conditions. So, homology modelling of proteins was performed (to address a range of representative subsets and to maximize the percentage similarity of sequence) by the SWISS-MODEL server [36].

Identification of Properties of the Target Protein

The physical and chemical parameters of the target protein structure were determined by the ProtParam server [37]. The secondary structures of target proteins were predicted by a self-optimized prediction method (SOPMA) [38]. SOSUI (engine ver. 1.11) [39] was used to determine whether the drug target is a soluble or a transmembrane protein. The crystal three-dimensional (3-D) structure of proteins was downloaded from the website Swiss-Model-Server [36]. SWISS-MODEL is a computerized homology modelling server that was used to superimpose proteins to deduce structural alignments and compare their active sites. The selected proteins- Model Quality Estimation (QMEAN Scores), sequence identity, coverage, method, and resolution details were determined (Table 1).

Table 1: QMEAN Scores for the model protein generated by using SWISS- MODEL server.

Target/ Receptor	Template	Model Quality Estimation (QMEAN Scores)	Sequence Identity	Coverage	Method	Resolution
AMPK 1	**4rer.1.A**	**0.68 ± 0.05**	99.07	0.97	X-ray	4.05Å
AMPK 2	7myj.2.A	0.73 ± 0.05	99.82	1	X-ray	2.95Å
DPP-4	2qt9.1.A	0.91 ± 0.05	99.87	1	X-ray	2.10Å
α-Glucosidase	3ton.1.A	0.83 ± 0.05	98.99	0.32	X-ray	2.95Å
PPARγ receptor	3e00.1.B	0.73 ± 0.05	100	0.8	X-ray	3.10Å

The protein structure against a background of phi-psi probabilities was validated by Ramachandran Z-score and Ramachandran plot - Zlab [40]. The active site and its functional domain were identified by CASTp 3.0 software [41].

Preparation of Target Proteins

The energy of the target proteins was minimized by Swiss-Pdb Viewer (aka DeepView) v 4.1.1 [42]. It is used to superimpose proteins to construct structural alignments and judge their active sites or any other related parts and to obtain H-bonds, mutations in amino acids, angles and distances connecting atoms. With the help of UCSF Chimera software [43] hydrogen and charges were added, its molecular torsion, degree of freedom and stereo-chemical variation were adjusted, followed by computation of gasteiger charges were done and the file was saved in PDB-Format. Chimera is an extensible molecular modelling system. The target protein grid was developed by using Chimera and Auto Dock Vina tool [44] with grid dimensions 20Å, 20Å, 20Å and the grid box was set at -76.407, -36.793, 13.714 for AMPK1; -36.303,-82.337, -22.555 for AMPK2; -7.759, 55.202, 45.807 for DPP4; 19.717,-23.55, 34.849 for alpha glucosidase; -2.406, 32.019,17.164 for PPARγ in X, Y and Z coordinates [41].

Selection of Ligands and Library Preparation

Identification of *C. roseus* metabolites having antihyperglycemic properties was selected with the help of a literature survey. Vindoline alkaloids (CID: 260535) and their similar structures were selected for the study [27,28,32]. Compound libraries were prepared for 21 compounds (see Table 6). As a control, antidiabetic drugs Metformin (CID: 4091), Vildagliptin (CID: 6918537), Acarbose (CID: 445421), Pioglitazone (CID: 4829) were selected. 21 components were identified, and 4 control SDF files were downloaded from the PubChem [45] database. Their SDF file format was converted into a PDB file by Open Babel software [46].

Table 2: Library of vindoline alkaloid their similar structures and control drug (PubChem CID).

Vindoline alkaloid their similar structures (PubChem ID)				Control
CID: 260535	CID: 25203293	CID: 129316872	CID: 11969850	Metformin (CID: 4091)
CID: 16667702	CID: 24728631	CID: 124040752	CID: 5459818	Vidagliptin (CID: 6918537)
CID: 16596	CID: 11953805	CID: 40473139	CID: 3081522	Acarbose (CID: 445421)
CID: 129320270	CID: 425978	CID: 25203244	CID: 439783	Pioglitazon (CID: 4829)
CID: 25203805	CID: 260534	CID: 12444852	CID: 179551	
			CID: 132599668	

ADMET and Drug Likeness Property Prediction

All library compounds drug-likeness properties were determined by the software OSIRIS property explorer [47] and DruLiTo (Drug-likeness rules) tool [48]. The drug's likeness properties of compounds were tested by parameters like solubility (LogS) estimation, Total polar surface area (TPSA), CLogP calculation (Lipinski rule), molecular mass and an active fragment of the compound, and drug score. Pharmacokinetic properties of compounds are predicted by their oral and gastrointestinal absorption, distribution, metabolism, and excretion (ADME) possibilities in the body. The pharmacodynamics activities of a compound were predicted by its bioavailability at the target side, blood-brain barrier crossing possibility, toxicity, carcinogenicity etc.

Preparation of Ligands

The ligands were prepared by using Avogadro 1.2. on-win 32 [49]. The tool is used for force field and geometry optimization. The UCSF Chimera [46] tool was used for hydrogen addition, charge addition, and ionization of

lead compound followed by adjustment of torsion, degree of freedom and stereo-chemical variation of ligand and then gasteiger charges were calculated and finally, the file was saved in a PDB file format.

Docking Studies and MD Stimulation

In chimera software, the prepared target protein (pdb file) and prepared ligand (pdb file) were opened. Surface binding analysis of them was performed with the help of the Grid, having sizes of 20 Å, 20 Å, 20Å. The Vina result score (energy value) was recorded, and the docked file was saved in pdbqt format. Receptor-ligand interactions were identified and visualized by BIOVIA discovery studio visualizer 4.5 [50]. It provides *in-silico* techniques related to molecular mechanics, free energy calculations, biotherapeutics development ability and more in the general environment. Bond details and docking surfaces were analyzed. iMOD server was used for MD simulation study and assessment of docking complexes. It customizes the binding affinity of target ligands based on the charge ratio and force field [51]. The server explores the joint motions of macromolecules (proteins, nucleic acids) by normal mode analysis (NMA). The MD simulation is supportive in screening, evaluation of docked complexes and with respect to binding free energy, giving information about correct rank of docking score functions [52].

RESULTS

Metabolites Compound Library Analysis and Active Ligand Identification of C. Roseus

With extensive bibliographic research, vindoline alkaloids and their similar structures were selected for the study. At present, 21 compounds have been identified and downloaded from the PubChem [45] database (Table 2). All the compounds were tested for ADMET and drug-likeness properties. Among all compounds, only vindoline alkaloid (CID: 425978) passed the screening test and was selected for lead preparation.

Target Protein Analysis and Active Site Identification

Selected drug targets are listed in (Table 3). The target 5'-AMP-activated protein kinase catalytic subunit alpha-1 (AMPK1, UniProt ID Q13131·AAPK1_HUMAN) is an enzyme (EC: 2.7.11.1). Similarly, 5'-AMP-activated protein kinase catalytic subunit alpha-2 (AMPK2, UniProt ID P54646·AAPK2_ HUMAN) EC: 2.7.11.1, Dipeptidyl peptidase 4 (DPP4, UniProt ID P27487 DPP4_HUMAN) EC: 3.4.14.5; and the α-Glucosidase (UniProt ID-O43451 MGA_HUMAN) belongs to Maltase-glucoamylase (EC: 3.2.1.20) are enzyme protein. Whereas Peroxisome proliferator-activated receptor gamma (PPARγ, UniProt ID P37231 · PPARG_HUMAN) is a nuclear receptor, made up of 505 amino acids.

Table 3: Physiochemical property of target proteins (uniprot and protparam value).

Proteins	Uniprot/PubMed ID	Length (Amino acid)	Molecular weight	pI	Instability index	Aliphatic index	Grand average of hydropathicity (GRAVY)	Extinction coefficients (M-1 cm-1, at 280 nm)	Estimated half-life (mammalian reticulocytes, in vitro)
AMPK	AAPK1_HUMAN (Q13131)	559AA	64009.23	8.32	49.44	84.03	-0.461	60905	30 hours
	AAPK2_HUMAN (P54646)	552AA	62319.61	7.65	49.2	85.11	-0.295	53290	30 hours
DPP-4	DPP4_HUMAN (P27487)	766 AA	88278.63	5.67	43.35	80.29	-0.34	198940	30 hours
α-glucosidase	MGA_HUMAN (O43451)	2,753 AA	312022.39	5.21	38.54	78.08	0.336	590100	30 hours
PPARγ	PPARG_HUMAN (P37231)	505AA	57620.15	5.61	50.2	86.32	-0.308	32320	30 hours

Physiochemical properties of the proteins of AMPK, DPP-4, α-glucosidase, and PPARγ have been revealed by its sequence analysis and it talks about the stability index, theoretical PI value, the aliphatic index, Grand average of hydropathicity (GRAVY), extinction coefficient, and estimated half-live computed as shown in Table 3. All these results show that the target proteins were stable macromolecules. The secondary structure of the target protein uncovered the maximum presence of the alpha helix, random coil, extended and the beta-strand on it (Table 4). AMPK2, DPP-4, and α-Glucosidase have transmembrane helices whereas AMPK1 and PPARγ are soluble

proteins (Table 5). The distribution of the torsion angles (phi (φ) and psi (ψ)) of the protein backbone of the target protein validates their structure (Table 6). The Castp web server result shows surface features and functional regions on three-dimensional structures of proteins and the presence of amino acids in the active site of the protein. In the target protein active site contains acidic, basic and neutral types of amino acids. Arg199 of AMPK1, Glu264 of AMPK2, Lys554 of DPP4, Asp2175 of α-glucosidase, and Asn403 of PPARγ were randomly selected at the active site of target protein because they play vital roles in catalytic activity and its coordinate has low binding potential energy. Followed by molecular docking analysis was performed between control drugs/*C. roseus* (Vindoline, CID: 425978) active compounds with the target protein.

Table 4: Secondary structure detail of target protein (SOPMA result).

Proteins	Sequence Length	Alpha Helix (Hh)	310 Helix (Gg)	Pi Helix (Ii)	Beta Bridge (Bb)	Extended Strand (Ee)	Beta Turn (Tt)	Bend Region (Ss)	Random Coil (Cc)	Ambiguous states	Other States
AMPK1	559	30.95%	0.00%	0.00%	0.00%	17.35%	6.80%	0.00%	44.90%	0.00%	0.00%
AMPK2	552	27.72%	0.00%	0.00%	0.00%	17.39%	8.15%	0.00%	46.74%	0.00%	0.00%
DPP-4	766	18.15%	0.00%	0.00%	0.00%	29.63%	6.53%	0.00%	45.69%	0.00%	0.00%
α-Glucosidase	2753	18.99%	0.00%	0.00%	0.00%	25.67%	6.85%	0.00%	48.49%	0.00%	0.00%
PPARγ	505	45.94%	0.00%	0.00%	0.00%	11.29%	5.54%	0.00%	37.23%	0.00%	0.00%

Table 5: SOSUI prediction about nature of target protein.

Receptor	Protein Nature	No	Region	Transmembrane Seq	Type
AMPK1	Soluble Protein				
AMPK2	Membrane Protein	1	6-28	KVLLGLLGAAALVTIITVPVVLL	Primary
DPP4	Membrane Protein	1	6-28	KVLLGLLGAAALVTIITVPVVLL	Primary
α-glucosidase	Membrane Protein	1	12-34	LEIVLSVLLLVLFIISIVLIVLL	Primary
PPARγ	Soluble Protein				

Table 6: Ramachandran Z-score and Ramachandran plot of target proteins.

S No	Receptor	Ramachandran Z-Score	Ramachandran Plot		
1	**AMPK1 (Template-4rer.1.A)**	**-3.583**	Highly Preferred Observations (Green Crosses)	463 (95.859%)	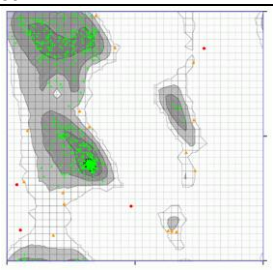
			Preferred observations (Brown Triangles)	16 (3.313%)	
			Questionable observations (Red Circles)	4 (0.828%)	
2	**AMPK2 (Template-7myj.2.A)**	**-2.135**	Highly Preferred Observations (Green Crosses)	464 (96.667%)	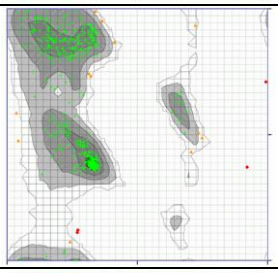
			Preferred Observations (Brown Triangles)	12 (2.500%)	
			Questionable Observations (Red Circles)	4 (0.833%)	
3.	**DPP4 (Template-2qt9.1.A)**	**-1.912**	Highly Preferred Observations (Green Crosses)	1298 (98.333%)	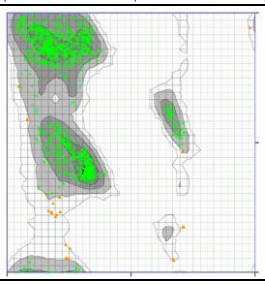
			Preferred Observations (Brown Triangles)	22(1.667%)	
			Questionable Observations (Red Circles)	0(0.000%)	
4	**α-Glucosidase (Template-3ton.1.A)**	**-3.603**	Highly Preferred Observations (Green Crosses)	733 (95.692%)	

			Preferred Observations (Brown Triangles)	32 (4.178%)	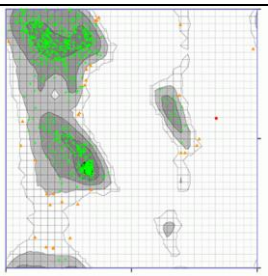
			Questionable Observations (Red Circles)	1 (0.131%)	
5	**PPARγ (Template-3e00.1.B)**	**-3.610**	Highly Preferred Observations (Green Crosses)	325 (95.870%)	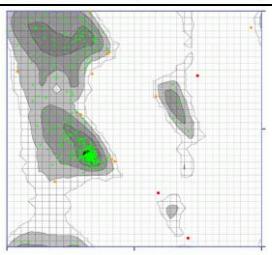
			Preferred Observations (Brown Triangles)	11 (3.245%)	
			Questionable Observations (Red Circles)	3 (0.885%)	

ADMET and Drug Likeness Prediction

All the selected library compounds passed the Lipinski rule and most of the compounds passed the Ghose filter, BBB likeness, Veber filter, and MDDR test but only one compound was qualified for the toxicity test and then it was taken for testing the Drug likeness and Drug-score. The best ligand (Table 7) and control results of the OSIRIS Property Explorer are shown in (Table 8). The tool generates values related to CLogP (O/W): Logarithm of partition coefficient between n-octanol and water; logS: the logarithmic value of aqueous solubility; TPSA: Topological polar surface area. Values obtained by using software for qualified biomolecule CID: 425978 are within standard criteria, whereas rest 20 compounds had ambiguous configurations at the stereo centre because of 2 parallel bonds/ unbalanced atom charge. ADMET (Absorption, Distribution, Metabolism, Excretion and Toxicity) features were identified by DruLiTo tools and OSIRIS Property Explorer. Toxicity risk was computed for mutagenic, carcinogenic; irritation and reproductive properties and the best result was indicated by the Green colour. For Vindoline alkaloid (CID: 425978) toxicity test result is green indicating that the compound qualifies as non-mutagenic, noncarcinogenic, non-irritation and not reproductive or within standard criteria. Non-carcinogenic and non-mutagenic profile shows that there would be no accumulation of biomolecules in the human body, and it would not cause cancer or mutation in the future if used for long-duration treatment. Also, the non-irritating property shows that it might have no gastrointestinal problem, vomiting, diarrhoea etc. A value of CLogP = 1.32, means, the compound has great hydrophilicity and can absorbed effortlessly by the cells, which has a good possibility of absorption in the gastrointestinal tract upon oral administration. Log S (solubility) = -3.12 mol/lit means the compound has good absorption and distribution characteristics. Molecular weight = 456 shows that biomolecule has high activity on a biological target and a high possibility to reach the place of action. TPSA = 88.54 means to have a high topological polar surface area for activity; Drug likeness = + 3.95, the positive value of drug-likeness representing molecules containing predominant fragment having a biological activity or drug-likeness property; Drug-score = 0.74 shows that compound has a higher possibility to qualify for a drug; and blood-brain barrier (BBB) likeness test by DruLiTo tool indicated by the red colour which means it may cross BBB. Overall DruLiTo and Osiris software result show that the compound has good drug efficacy and become a potential drug candidate and can be used for ligand preparation.

Table 7: Ligand/lead details like IUPAC name, molecular weight and 3D structure.

Ligand	PubChem ID	IUPAC name	Molecular weight (g/mol)	3D Image
Vindoline	CID: 425978	Methyl 11-acetyloxy-12-ethyl-10-hydroxy-5-methoxy-8-methyl-8,16-diazapentacyclo[10.6.1.01,9.02,7.016,19]nonadeca-2(7),3,5,13-tetraene-10-carboxylate	456.5	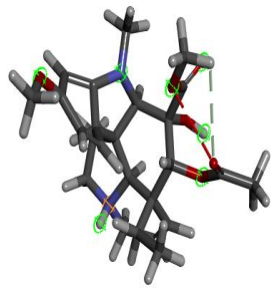

Table 8: ADMET and Drug likeness prediction.

Compound Name	Title (PubChem CID	Toxicity Risk	CLogP	Log S (Solubility)	Molecular Weight	TPSA	Drug Likeness	Drug Score	BBB
Vindoline	CID: 425978	G	1.32	-3.12	456	88.54	3.95	0.74	Fail
Metformin	CID: 4091	G	-1.54	-0.13	129	91.49	1.21	0.88	Pass
Vildagliptin	CID: 6918537	G	0.56	-2.67	303	76.36	0.66	0.75	Pass
Acarbose	CID:445421	G	-7.18	0.59	645	321.1	-7.4	0.29	Fail
Pioglitazone	CID: 4829	G	3.08	-3.83	356	93.59	5.02	0.76	Pass

Abbreviation: CLog P (O/W): Logarithm of partition coefficient between n-octanol and water, logS: Aqueous solubility, TPSA: Topological polar surface area.

Molecular Docking Analysis of Control Drugs (Metformin) and C. roseus (Vindoline, CID: 425978) Active Compounds with AMPK Target

AMPK1 - Ligand Interaction

Metformin belongs to the Biguanides family and acts as an activator of AMPK [53,54]. In computational drug discovery, intermolecular interaction in the molecular docked pose of Metformin (control drug) confirmed its binding to the active site of catalytic subunit alpha-1of 5'-AMP-activated protein kinase (AMPK1) target of the human. Figure 2A - Figure 2D shows the binding of metformin with AMPK1 chain A, catalytic pocket residue ARG199 and interactions between them. They interact with 2 Conventional H-bond interactions with Leu200, 6 attractive Charge interactions with GLU205, GLU194, one Salt Bridge: Attractive Charge interaction with GLU205, 2 Pi-Cation interactions with PHE180 and one unfavourable Donor-Donor interaction with ALA202. The binding affinity energy of the metformin with AMPK1 is -4.0 kcal/mol (Table 9).

Table 9: Molecular docking analysis: Binding energy and the type of molecular interaction between Metformin (control drugs) and active compound of *C. roseus* Vindoline (CID: 425978) against target AMPK1.

Compounds	Vina Score/Binding Affinity (kcal/mol)	ligand	Distance(Å)	Target Protein	Category	Type of Interaction
AMPK1-Metformin (Control)	-4	UNL1:H	2.45	A: LEU200: O	Hydrogen Bond	Conventional H-bond Interaction
		UNL1:HN2	2.2	A: LEU200: O	Hydrogen Bond	Conventional H-bond Interaction
		UNL1:N	5.57	A:GLU205:OE2	Electrostatic Attraction	Attractive Charge Interaction
		UNL1:N	4.27	A:GLU205:OE2	Electrostatic Attraction	Attractive Charge Interaction
		UNL1:N	3.95	A:GLU205:OE2	Electrostatic Attraction	Attractive Charge Interaction
		UNL1:N	3.06	A:GLU194:OE2	Electrostatic Attraction	Attractive Charge Interaction
		UNL1:N	4.79	A:GLU194:OE2	Electrostatic Attraction	Attractive Charge Interaction
		UNL1:N	2.96	A:GLU194:OE2	Electrostatic Attraction	Attractive Charge Interaction
		UNL1:H	1.84	A:GLU205:OE2	Electrostatic Attraction	Salt Bridge; Attractive Charge Interaction
		UNL1:N	4.16	A:PHE180	Non-Covalent Molecular Interaction	Pi-Cation Interaction
		UNL1:N	4.91	A:PHE180	Non-Covalent Molecular Interaction	Pi-Cation Interaction
		UNL1:H	2.55	A:ALA202:HN	Intrinsic Interactions	Unfavorable Donor-Donor Interaction
AMPK1-Vindoline (Test)	-6.3	UNL1:NH	2.3	A:LEU462:O	Hydrogen Bond	Conventional H-bond Interaction
		UNL1:O	2.31	A:ARG 182:HH22	Hydrogen Bond	Conventional H-bond Interaction
		UNL1:C	3.62	A: GLY198:O	Hydrogen Bond	Carbon H-bond Interaction
		UNL1:C	3.59	A: GLY198:O	Hydrogen Bond	Carbon H-bond Interaction
		UNL1:C	3.56	A:GLN461:OE1	Hydrogen Bond	Carbon H-bond Interaction
		UNL1	5.2	A:LEU200	Hydrophobic	Alkyl Interaction
		UNL1	5.47	A:TYR463	Hydrophobic	Pi-Alkyl Interaction

Abbreviation: UNL: *C. roseus* active compounds, LEU: Leucine, GLU: Glutamic acid, PHE: Phenylalanine, ALA: Alanine, ARG: Arginine, GLY: Glycine, GLN: Glutamine, TYR: Tyrosine.

Figure 2E - Figure 2H shows the binding of Vindoline (CID: 425978) with AMPK1 chain A, catalytic pocket residue ARG199 and interactions between them. The bioactive compound, vindoline (CID: 425978) molecular docked pose shows strong intermolecular interaction and is attached to the active site of the AMPK1 by

noncovalent interaction and has minimum binding affinity energy is -6.3 kcal/mol. Among noncovalent bonds there are 2 conventional H-bond interactions with ARG182, LEU462; 3 Carbon H-bond interactions with GLY198, GLN461, one Alkyl interaction with LEU200 and one Pi-Alkyl interaction with TYR463 (Table 9).

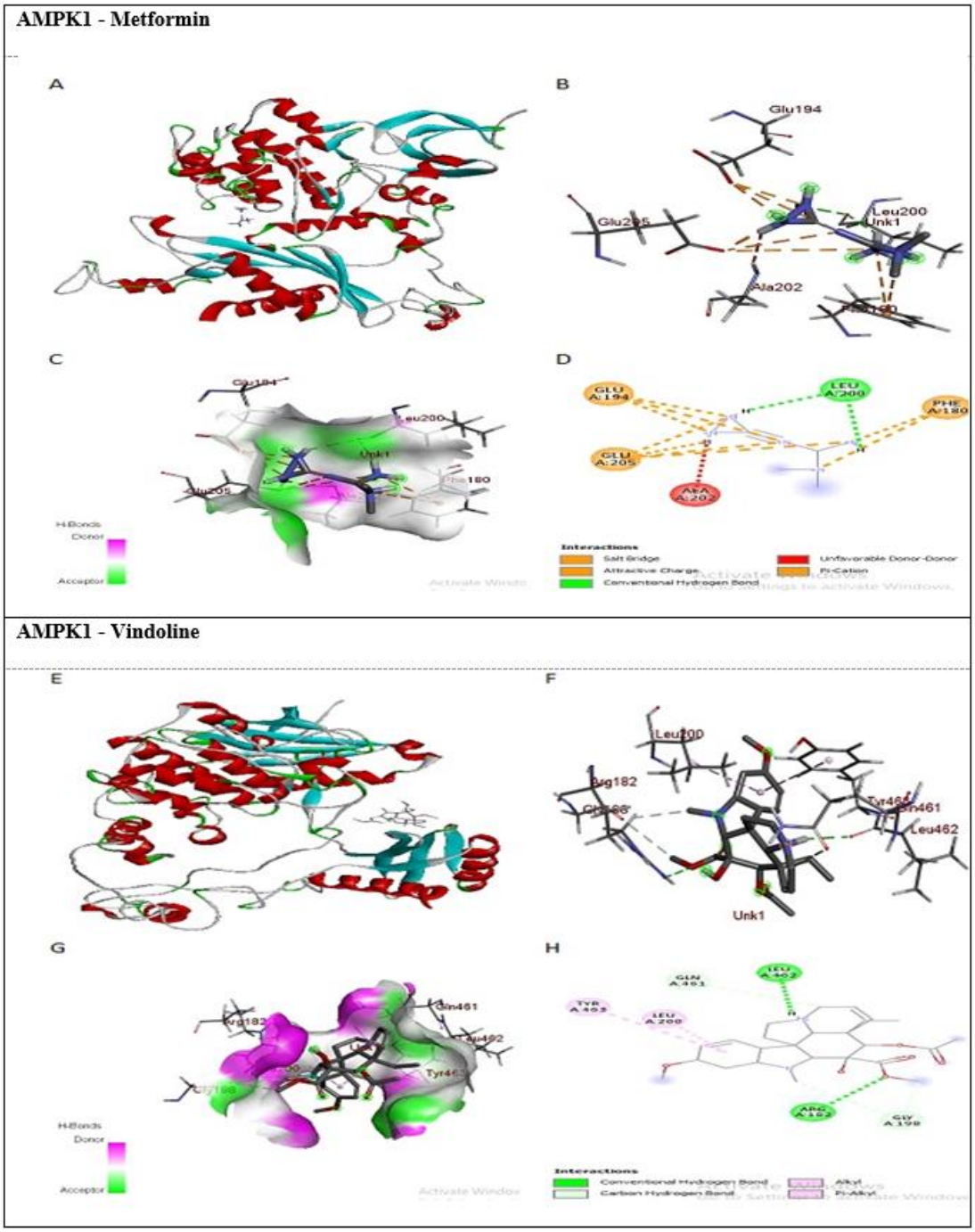

Figure 2: Molecular docking studies of bonding interaction between AMPK1 target protein and Control ligand (Metformin) and test ligand (Vindoline). **(A)** Docking pose of metformin in AMPK1, **(B)** Metformin interaction with different target amino acids residue of AMPK1, **(C)** 3-D (three dimensional) diagram based on hydrogen bond donor and acceptor characteristics of AMPK1 target and Metformin ligand, **(D)** 2-D (two dimensional) diagram of highlighting different bonding interactions between AMPK1 and metformin. Similarly, **(E)** Docking pose of vindoline in AMPK1, **(F)** Vindoline interaction with different target amino acids residue of AMPK1, **(G)** 3-D (three dimensional) diagram based on hydrogen bond donor and acceptor characteristics of AMPK1 target and vindoline ligand, **(H)** 2-D (two dimensional) diagram of highlighting different interactions between AMPK1 and vindoline.

Molecular dynamics (MD) simulation analysis by iMODS supports the AMPK1-vindoline docked complex (ID: 0706165201010) (Figure 3). Figure 3A is related to the deformability graph, it shows which residues are deforming themselves for interaction. There are 15 hinges (2 hinges at maximum deformability (1), one at 0.8, 3 between 0.6 to 0.8, and 9 between 0.4 to 0.6), the point at which the target and ligand interact. It supports good, docked complexes binding. B-Factor Mobility/NMA mobility graph (Figure 3B) shows a correlation between the actual experimental result (PDB graph) and simulation result (NMA). The eigenvalue of AMPK1 and vindoline complex is 3.69e-06 (Figure 3C). It means that 3.69e-06 energy is required for interaction or deformation of the structure. (Figure 3D) represents Variance plot, bars show the individual frequency (purple colour) is lower than cumulative frequency (green colour) of residues. Figure 3E is a Covariance plot, where red colour around the central line, supporting that residual index is positively correlated/ positive correlation between AMPK1 target and vindoline ligand. The elastic network (Figure 3F) is light grey around the central line, supports that interaction between them is flexible and less chance of ligand coming out from the active site of AMPK1.

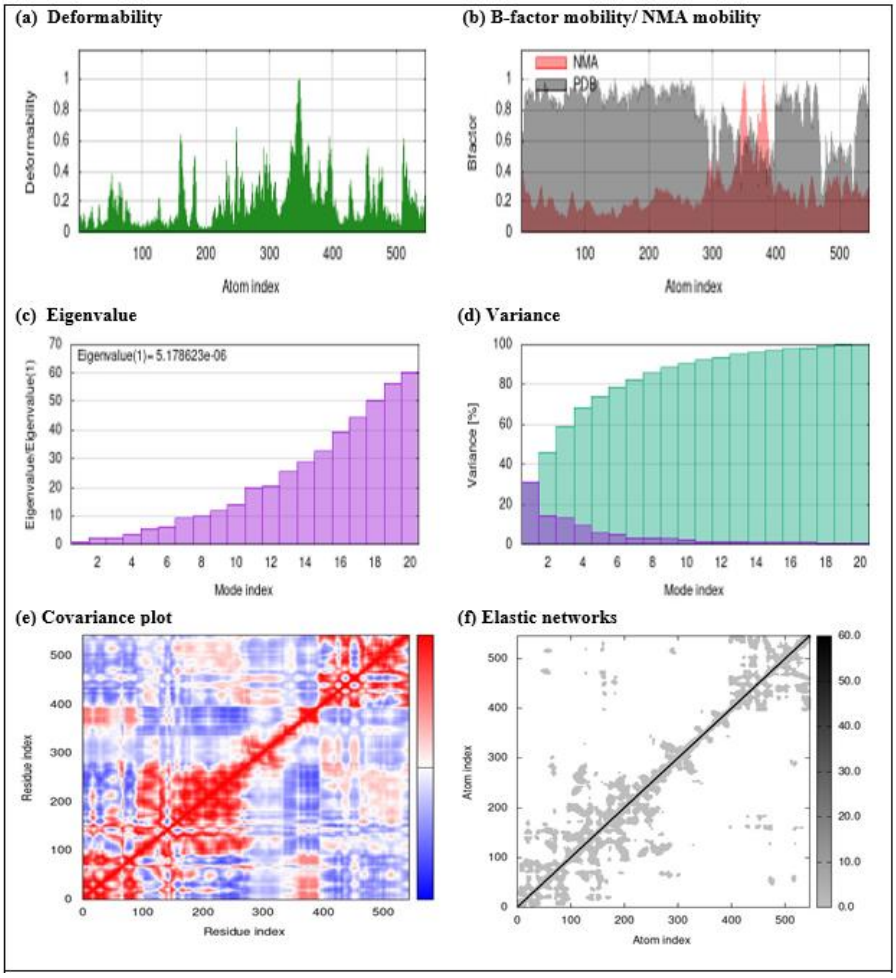

Figure 3: MD simulations results of docked complex AMPK2-Vindoline (ID: 0706165730293).

MD simulation and analysis and binding affinity (-6.3 kcal/mol) of the AMPK1-vindoline (CID: 425978) is supporting about more strong and stable binding between them in comparison to metformin with AMPK1 (-4.0 kcal/mol). The lower free energy of binding of vindoline may be due to comparatively stronger non-covalent interaction at the lower distance between the bioactive compound and AMPK1.

AMPK2 - Ligand Interaction

Intermolecular interaction in the molecular docked position of the Metformin (control drugs) confirmed that they interact with the active site of catalytic subunit alpha-2 of 5'-AMP-activated protein kinase (AMPK2) chain A, catalytic pocket residues GLU264. The binding of AMPK2 with metformin is with 4 conventional H-bond interactions with ASP261, HIS247, THR243; one Carbon H-bond interaction with ASP261; 2 Attractive Charge interactions with ASP261 as shown in (Figure 4A - Figure 4D). The binding affinity energy of the metformin with AMPK2 is -4.2 kcal/mol (Table 10). AMPK2 promotes glucose uptake internalization and recycling of the insulin receptor (INSR).

The minimum binding affinity conformer molecular docked pose (Figure 4E - Figure 4H) of the *C roseus* active compound, vindoline (CID: 425978) binding, has confirmed that it also definitely goes and binds to the active site of the AMPK2 chain A, around catalytic pocket residues GLU264 with two conventional H-bond interactions ARG263, two Carbon H-bond interactions with ARG263, LYS260, 2 Alkyl interactions with LEU272, ARG263; one Attractive Charge interaction with GLU279 and one unfavourable Acceptor-Acceptor Interaction with ASP280 (Table 10).

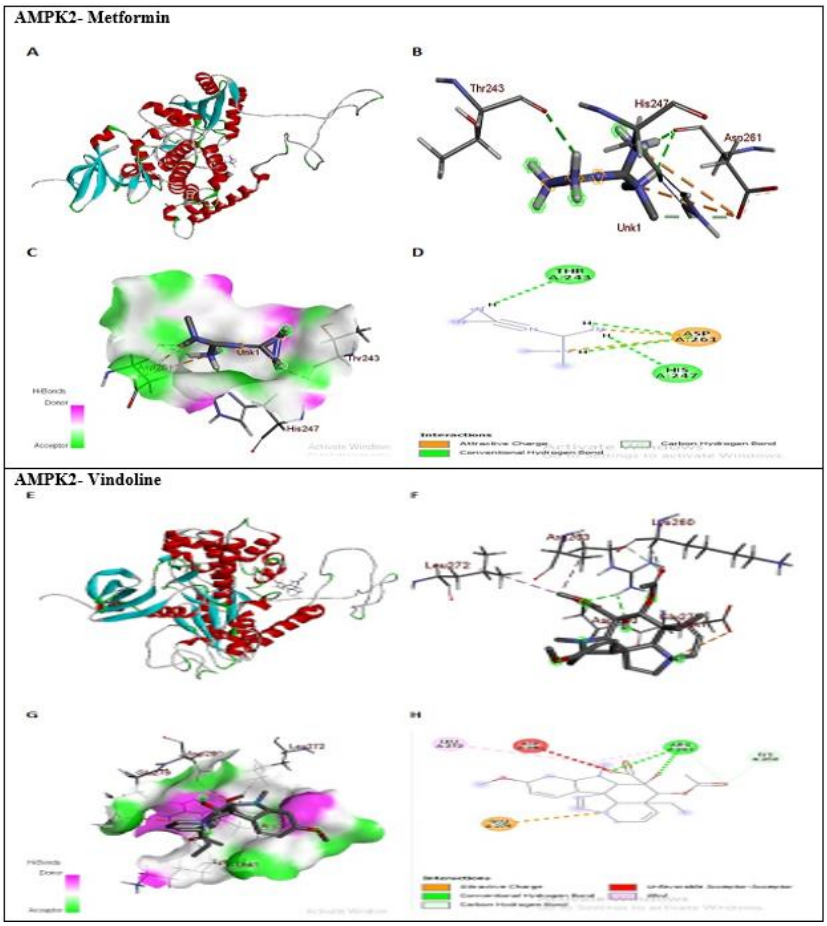

Figure 4: Molecular docking studies of AMPK2 target protein and Control ligand (Metformin) and test ligand (Vindoline). **(A)** docking pose view of metformin with AMPK2 in its catalytic region **(B)** is showing bonding interaction between target amino acids residue of AMPK2 and control ligand **(C)** 3-D (three dimensional) diagram interaction analysis of H-surface of target and metformin **(D)** 2-D (two dimensional) diagram interactions between AMPK2 and metformin. Similarly, **(E)** Docking pose of vindoline in AMPK2, **(F)** Vindoline ligand interaction with different amino acids residue of target AMPK2, **(G)** 3-D (three dimensional) interaction diagram based on hydrogen bond donor and acceptor characteristics of AMPK2 surface and Vindoline ligand, **(H)** 2-D (two dimensional) diagram represents different interactions between AMPK2 and vindoline.

Table 10: Molecular docking analysis: Binding energy and the type of molecular interaction of control drugs and active compound of *C. roseus* against target AMPK2. UNL: *C. roseus* active compounds, ASP: Aspartic acid, HIS: Histidine,

Compounds	Vina Score/Binding Affinity (kcal/mol)	Ligand	Distance (Å)	Target Protein	Category	Type of Interaction
AMPK2-Metformin (Control)	-4.2	UNL1:HN	2.33	A: ASP261:O	Hydrogen Bond	Conventional H-bond interaction
		UNL1:H	2.11	A: ASP261:O	Hydrogen Bond	Conventional H-bond Interaction
		UNL1:HN2	2.4	A:HIS247:ND1	Hydrogen Bond	Conventional H-bond Interaction
		UNL1:H	2.4	A: THR243:O	Hydrogen Bond	Conventional H-bond Interaction
		UNL1:C	3.54	A:ASP261:OD1	Hydrogen Bond	Carbon H-bond Interaction
		UNL1:N	4.45	A:ASP261:OD1	Electrostatic Attraction	Attractive Charge Interaction
		UNL1:N	5.18	A:ASP261:OD1	Electrostatic Attraction	Attractive Charge Interaction
AMPK2-Vindoline (Test)	-6.2	UNL1:O	2.21	A:ARG263:HH21	Hydrogen Bond	Conventional H-bond Interaction
		UNL1:O	2.29	A:ARG263:HH21	Hydrogen Bond	Conventional H-bond Interaction
		UNL1:O	2.8	A:ARG263:HD2	Hydrogen Bond	Carbon H-bond Interaction
		UNL1:O	2.62	A:LYS260:HA	Hydrogen Bond	Carbon H-bond Interaction
		UNL1:C	5.22	A:LEU272	Hydrophobic	Alkyl Interaction
		UNL1:C	3.87	A:ARG263	Hydrophobic	Alkyl Interaction
		UNL1:N	5.36	A:GLU279:OE2	Electrostatic Attraction	Attractive Charge Interaction
		UNL1:O	2.97	A:ASP280:OD1	Intrinsic Interactions	Unfavorable Acceptor-Acceptor Interaction

MD simulation by iMODS supporting that AMPK2 and vindoline complex (ID:0706165730293) is stable docked complex (Figure 5). Its deformability plot has 10 hinges (1 at maximum deformability (1), 2 between 0.6 to 0.8, and 7 between 0.4 to 0.6), which means 10 points of interactions between the target and ligand (Figure 5A). B-factor mobility shows that correlation between experimental PDB result and MD simulation NMA result (Figure 5B). Eigenvalue of the complex is 5.18e-06 (Figure 5C). Variance (Figure 5D), covariance (Figure 5E) and Elastic networks (Figure 5F) plot show that there is a presence of positive correlation and flexible interaction between target AMPK2 and Vindoline.

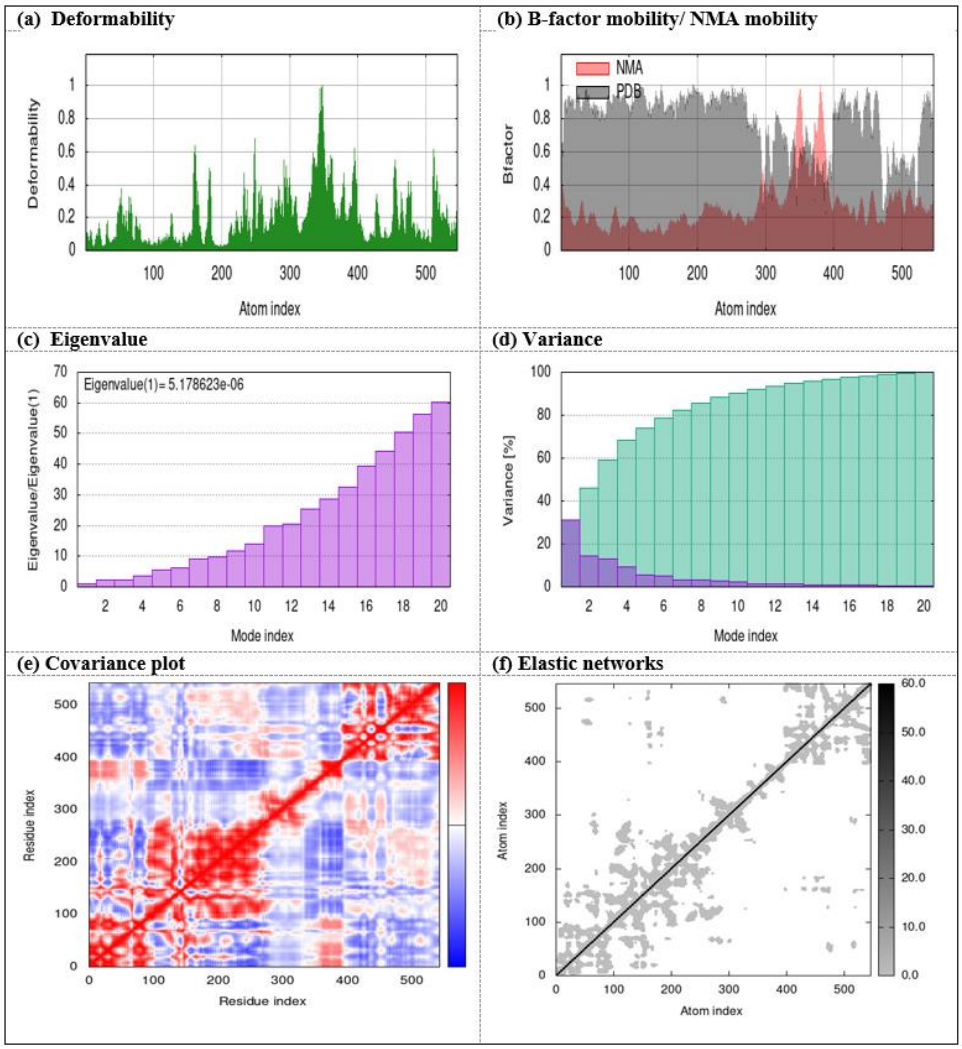

Figure 5: MD simulations results of docked complex AMPK2-Vindoline (ID: 0706165730293).

On comparing the binding affinity of metformin (-4.2 kcal/mol) with the binding affinity of vindoline (CID: 425978) on the AMPK2 target, we found that vindoline has a greater binding affinity energy than the control one with -6.2 kcal/mol. MD simulation result and binding free energy supports that the lead is a potent activator of AMPK2 so it may control and regulate hyperglycemia and its complications in a better way than the present antidiabetic drug.

Molecular Docking Analysis of Control Drugs (Vildagliptin) and Vindoline (CID: 425978) with the DPP4

The *In-silico* result of minimum binding affinity conformer of the molecular docked pose of the vildagliptin and DPP4 target interaction verified that binding to vildagliptin in the active site of the target protein of human (Figure 6) and 2D (two dimensional) plot. Vildagliptin binds with DPP4 chain B, around catalytic pocket residues LYS554 and interactions between them through 5 conventional H-bonds with TYR547, TYR666, ASN710, SER630, HIS740; one Carbon H-bond interaction with GLY741; one Pi -Donar H-bond interaction with TRP629; 2 Pi-Alkyl interactions with TRP629; one Attractive charge interaction with GLU205, one unfavourable positive-positive interaction with ARG125 (Table 11).

Table 11: Molecular docking analysis: Binding energy and the type of molecular interaction of control drugs and active compound of *C. roseus* against DPP4.

Compounds	Vina Score/Binding Affinity (kcal/mol)	Ligand	Distance (Å)	Target Protein	Category	Type of Interaction
DPP4-Vidagliptin (Control)	-6.7	UNL1:N	2.45	B:TYR666:HH	Hydrogen Bond	Conventional H-bond Interaction
		UNL1:N	2.66	B:TYR547:HH	Hydrogen Bond	Conventional H-bond interaction
		UNL1:O	2.87	B:ASN710:HD21	Hydrogen Bond	Conventional H-bond interaction
		UNL1:O	2.53	B:SER630:HG	Hydrogen Bond	Conventional H-bond Interaction
		UNL1:H	2.73	B:HIS740:O	Hydrogen Bond	Conventional H-bond Interaction
		UNL1:O	2.45	B:GLY741:HA1	Hydrogen Bond	Carbon H-bond Interaction
		UNL1:H	2.52	B:TRP629	Hydrogen Bond	Pi -Donor H-bond Interaction
		UNL1	4.29	B:TRP629	Hydrophobic	Pi-Alkyl Interaction
		UNL1	5.25	B:TRP629	Hydrophobic	Pi-Alkyl Interaction
		UNL1:N	4.57	B:GLU205:OE2	Electrostatic Attraction	Attractive charge Interaction
		1:UNL1:N	4.77	B:ARG125:NH2	Intrinsic Interaction	Unfavorable positive-positive Interaction
DPP4-Vindoline (Test)	-6.8	UNL1:O	2.74	B:LYS554:HZ3	Hydrogen Bond	Conventional H-bond Interaction
		UNL1:O	2.94	B:LYS554:HZ1	Hydrogen Bond	Conventional H-bond Interaction
		UNL1:C	3.71	B:ASP545:OD2	Hydrogen Bond	Carbon H-bond Interaction
		UNL1:C	3.8	B: VAL546: O	Hydrogen Bond	Carbon H-bond Interaction
		UNL1	5.35	B:TYR547	Hydrophobic	Pi-Alkyl Interaction
		UNL1:N	4.32	B:TRP629	Non-Covalent Molecular Interaction	Pi-Cation Interaction
		UNL1:N	4.81	B:TRP629	Non-Covalent Molecular Interaction	Pi-Cation Interaction

Abbreviation: UNL: C. roseus active compounds. UNL: C. roseus active compounds, TYR: Tyrosine, ASN: Asparagine, SER: Serine, HIS: Histidine, GLY: Glycine, TRP: Tryptophan, GLU: Glutamic acid, ARG: Arginine, LYS: Lysine, ASP: Aspartic acid, VAL: Valine.

The final minimal potential energy of molecular dock pose (Figure 6E - Figure 6H) for the vindoline and DPP4 target protein is -6.8kcal/mol and root mean square deviation (RSMD) = 0. The docking result establishes that they also definitely go and bind to the active site of the DPP4 chain B, around catalytic pocket residues LYS554 through 2 Conventional H-bond interactions with LYS554; 2 Carbon H-bond interaction with ASP545, VAL546; one Pi-Alkyl interaction with TYR547; 2 Pi-Cation interaction with TRP629 (Table 11).

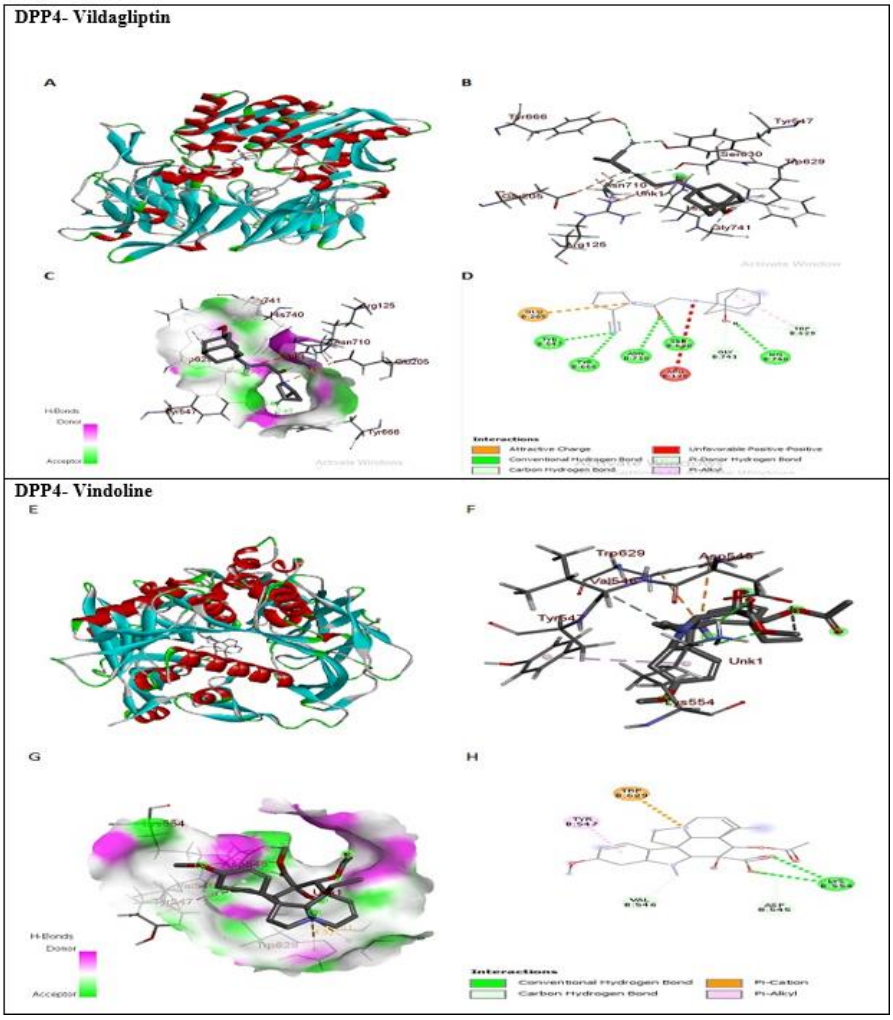

Figure 6: Molecular docking pose of DPP4 drug target and Control ligand (Vildagliptin) and test ligand (Vindoline). **(A)** Showing binding pose view of vildagliptin with DPP4 in its active site, **(B)** Represents interaction between target amino acids residue of DPP4 and control ligand, **(C)** 3-D interaction diagram is showing interaction of target H-surface and vildagliptin, **(D)** 2-D diagram representing interactions between vildagliptin and DPP4, **(E)** Binding pose view of test ligand vindoline with DPP4 in its catalytic region, **(F)** Denotes interaction between target amino acids residue of DPP4 and vindoline, **(G)** 3-D interaction illustration of hydrogen bond donor and acceptor characteristics of DPP4 surface and vindoline ligand, **(H)** 2-D diagram of interactions between DPP4 and vindoline.

MD simulation by iMODS between the docked complexes was used to check the elasticity and advancement in the protein structures as shown in (Figure 7). The deformability plot (Figure 7A) shows 17 hinges (1 at maximum deformability, 2 between 0.8- 1, 7 between 0.6-0.8 and 7 between 0.4- 0.6). The B-factor mobility plot shows overlapping conditions between experimental PDB and simulation NMA result (Figure 7B). The eigenvalue of the docked complex is 1.12e-04 (Figure 7C). The covariance plot (Figure 7E) and elastic networks plot (Figure 7F) show strong and flexible interaction between DPP4 and the vindoline complex.

On comparing the binding affinity of vildagliptin (-6.7 kcal/mol) with the binding affinity of vindoline (CID: 425978) (-6.8 kcal/mol) along with MD simulation result, we found that the biomolecules have a greater binding affinity with DPP4 target than control one so it may become a potent DPP-4 inhibitor and are a good therapeutic alternative for the treatment of the disease.

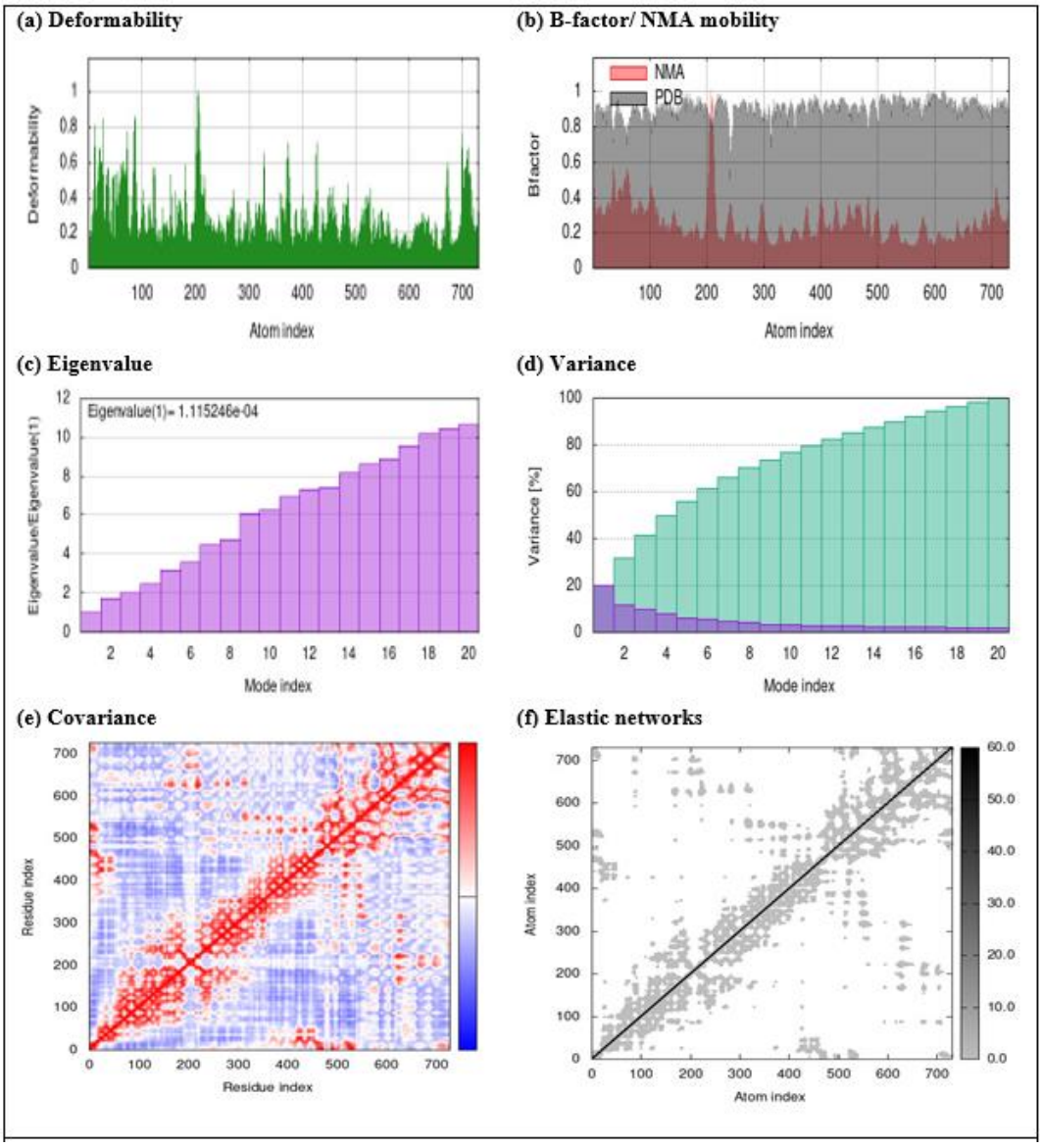

Figure 7: MD simulations results of docked complex DPP4-vindoline (ID: 0706170105690).

Molecular Docking Analysis of Acarbose (Control Drugs) and Vindoline (CID: 425978)

The intermolecular interaction of the molecular docked pose of the Acarbose (control drugs) demonstrated that they bind to the active site of the α-glucosidase protein of the human (Figure 8) and 2D (two-dimensional) plot. *In-silico* results show that acarbose binds with chain A of α-glucosidase around catalytic active site ASP2175 through 6 conventional H-bonds with TYR2147, ASP2177, MET2179, ARG2181, ASP2253, THR2482; one carbon H-bond with GLU2180; two Pi alkyl bond with TRP2251, TRP2265 and one unfavourable donor-donor interaction with TYR2147. The binding affinity energy and interaction details of the acarbose drugs are mentioned in Table 12. Acarbose, via a competitive inhibition mechanism, inhibits oligosaccharide binding to an alpha-glucosidase enzyme. The final minimal potential energy of molecular dock poses of acarbose, and the target protein is -6.7 kcal/mol.

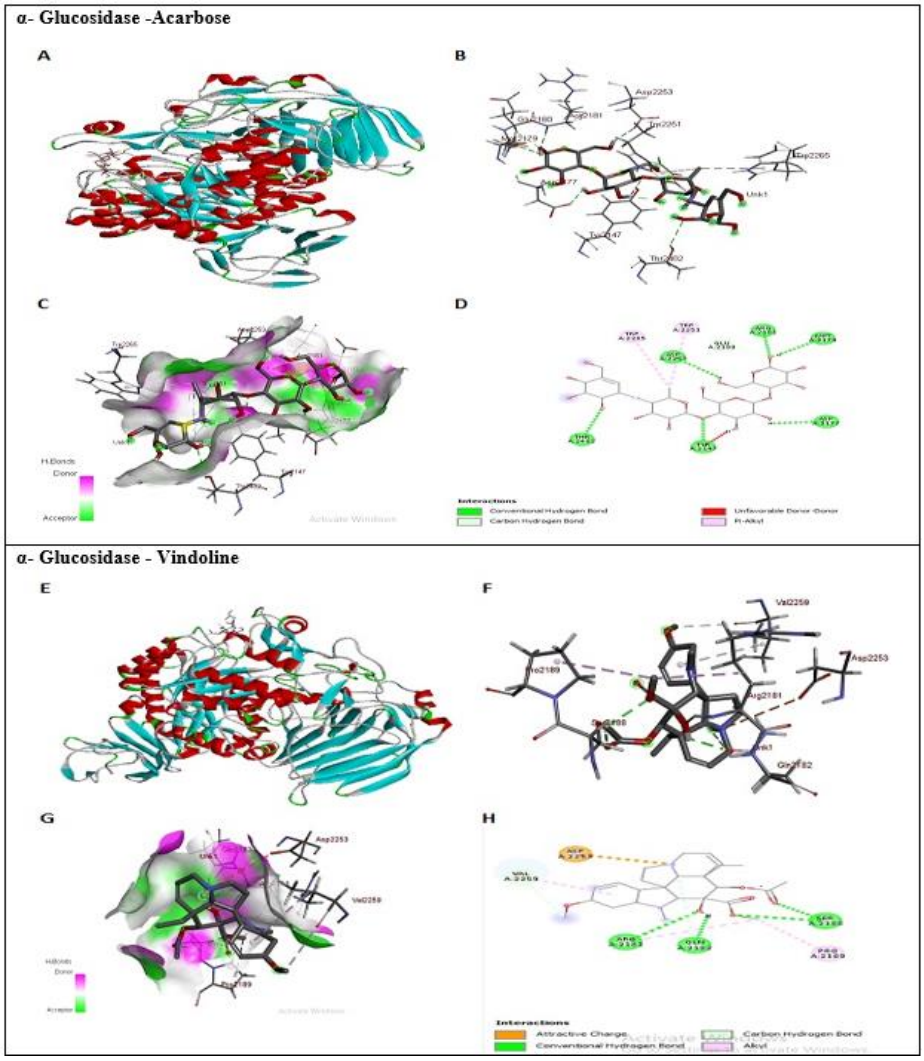

Figure 8: Molecular docking pose of α- Glucosidase target and Control ligand (Acarbose) and test ligand (Vindoline). **(A)** presentation docking pose view of acarbose with α- Glucosidase in its catalytic site, **(B)** represents interaction between amino acids residue of the target and control ligand, **(C)** 3-D image of interactions on the target H-surface and acarbose, **(D)** 2-D diagram representing interactions between acarbose and the target. Similarly, **(E)** interacting pose view of vindoline with α- Glucosidase in its catalytic active site, **(F)** signifies interaction between target amino acids residue of the target and test compound vindoline, **(G)** three-dimensional photograph showing hydrogen bond donor and acceptor characteristics of α- Glucosidase surface and interaction of vindoline ligand with it, **(H)** 2-D diagram of interactions of interactions between α- Glucosidase and vindoline.

Table 12: Molecular docking analysis: Binding energy and the type of molecular interaction of control drugs and active compound of *C. roseus* against alpha glucosidase.

Compounds	Binding Affinity (Kcal/mol)	Ligand	Distance(A°)	Receptor	Category	Type of Interaction
α- glucosidase Acarbose (Control)	-6.7	UNL1: O	3.02	A:THR2482:HG1	Hydrogen Bond	Conventional Hydrogen Bond Interaction
		UNL1: H	1.97	UNL1: O	Hydrogen Bond	Conventional Hydrogen Bond Interaction
		UNL1: O	2.03	A:TYR2147:HH	Hydrogen Bond	Conventional Hydrogen Bond Interaction
		UNL1: H	2.53	A:ASP2177:OD1	Hydrogen Bond	Conventional Hydrogen Bond Interaction
		UNL1: H	2.9	A:ASP2253:OD1	Hydrogen Bond	Conventional Hydrogen Bond Interaction
		UNL1: H	2.53	A: MET2179: O	Hydrogen Bond	Conventional Hydrogen Bond Interaction
		UNL1: O	2.03	A:ARG2181:HN	Hydrogen Bond	Conventional Hydrogen Bond Interaction
		UNL1: O	2.67	A:GLU2180:HA	Hydrogen Bond	Carbon Hydrogen bond Interaction
		UNL1: C	5.03	A:TRP2265	Hydrophobic	Pi-Alkyl Interaction
		UNL1: C	5.48	A:TRP2251	Hydrophobic	Pi-Alkyl Interaction
		UNL1: H	1.55	A:TYR2147:HH	Intrinsic Interactions	Unfavorable Donor-Donor Interaction
α- glucosidase -Vindoline (Test)	-6.8	UNL1:C	3.61	A:VAL2259	Hydrogen Bond	Carbon Hydrogen Bond Interaction
		UNL1:C	3.48	A:GLN2182:OE1	Hydrogen Bond	Carbon-Hydrogen Bond Interaction
		UNL1: O	2.81	A:ARG2181:HN	Hydrogen Bond	Conventional Hydrogen Bond Interaction
		UNL1: O	2.07	A:SER2188:HG	Hydrogen Bond	Conventional Hydrogen Bond Interaction
		UNL1: O	2.07	A:SER2188:HG	Hydrogen Bond	Conventional Hydrogen Bond Interaction
		UNL1	4.81	A:VAL2259	Hydrophobic	Alkyl Interaction
		UNL1:C	4.28	A:ARG2181	Hydrophobic	Alkyl Interaction
		UNL1:C	5.12	A:PRO2189	Hydrophobic	Alkyl Interaction
		UNL1:N	5.32	A:ASP2253:OD1	Electrostatic Attraction	Attractive Charge Interaction

Abbreviation: UNL: C. roseus active compounds, THR: Threonine, TYR: Tyrosine, ASP: Aspartic acid, MET: Methionine, ARG: Arginine, GLU: Glutamic acid, TRP: Tryptophan, VAL: Valine, GLN: Glutamine, SER: Serine, PRO: Proline.

C. roseus alkaloid vindoline (CID: 425978) binds strongly to the active site of the α-glucosidase target (Figure-8E - Figure 8H) through several non-covalent interactions (Table 12). The interactions between vindoline and α-glucosidase are three conventional H-bonds with ARG2181, SER2188; and 2 carbon H-bonds with GLN2182, VAL2259; 3 Alkyl interactions with ARG2181, PRO2189, VAL2259 and one Attractive Charge interaction with ASP2253. The binding affinity of acarbose (-6.7 kcal/mol) is lower than the binding affinity of vindoline (CID: 425978) -6.8 kcal/mol.

MD simulation of the docked complexes is showing about good binding interaction between target alpha-glucosidase and ligand vindoline (Figure 9). The deformability plot (Figure 9A) shows about 21 hinges (3 at maximum deformability (1), 3 between 0.6-0.8, and 15 between 0.4-0.6). The B-Factor mobility plot shows about overlapping condition between experimental PDB and simulation NMA result (Figure 9B). The eigenvalue (Figure 9C) of the complex is 1.96e-04, which means that much energy is required to deform the target structure. Whereas the covariance plot (Figure 9E), and elastic networks (Figure 9F) show a positive correlation between residues and flexible docked complex structure of alpha-glucosidase and vindoline.

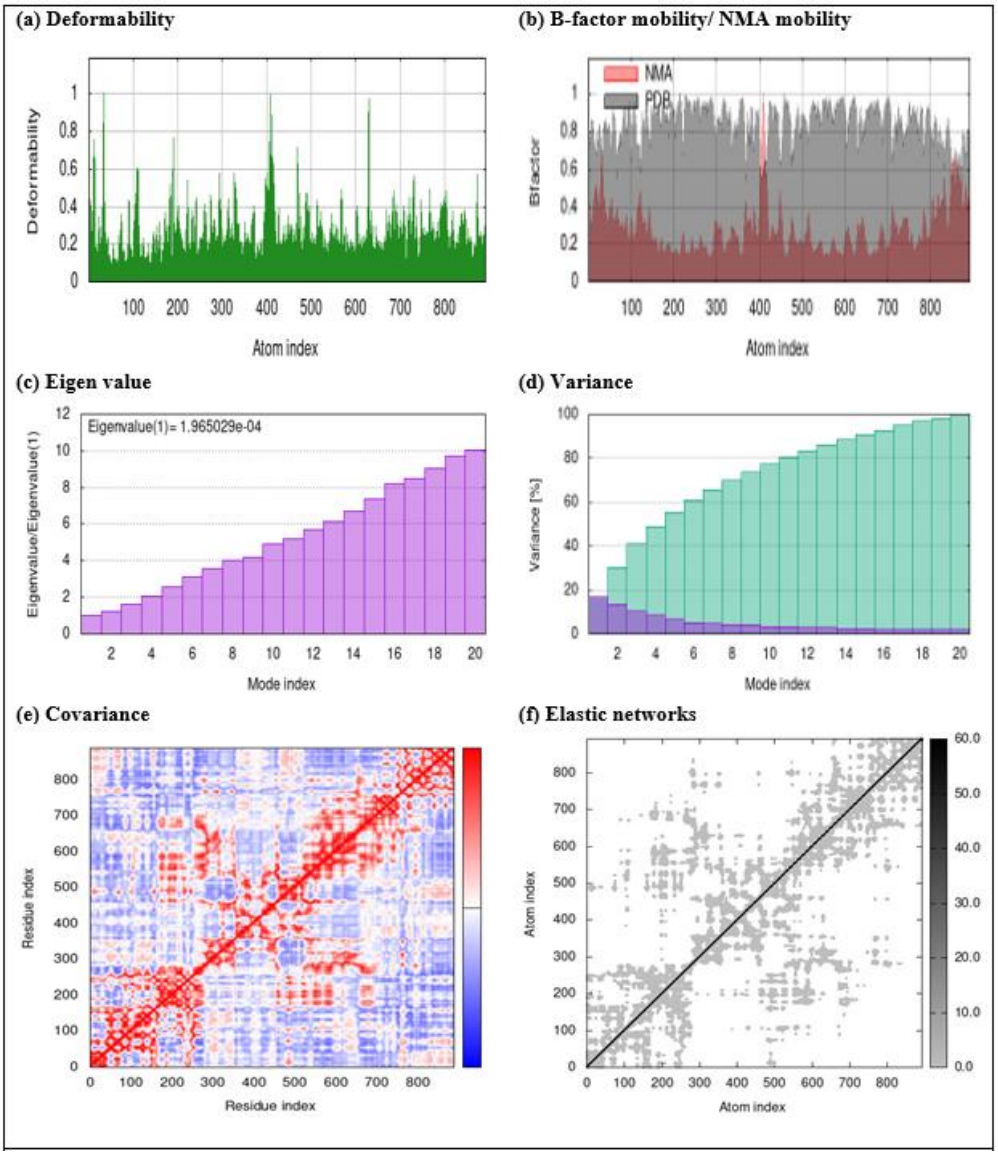

Figure 9: MD simulations results of docked complex alphaglucosidas-vindoline (ID:0706164743293).

The vina score and MD simulation result show that the alkaloid has a strong and higher binding free energy (-6.8 kcal/mol) than acarbose. This supports the alkaloid has a strong α-glucosidase enzyme inhibitory ability and better capability to regulate the rise in postprandial blood glucose level than acarbose.

Molecular Docking Analysis of Control Drugs (Pioglitazone) and C. roseus (Vindoline, CID: 425978) Active Compounds with the PPARγ

Computational calculation of the minimum binding affinity molecular docked pose of pioglitazone and PPARγ conformer established that pioglitazone binds with chain B, around catalytic site ASN403 of the PPARγ target (Figure 10). 3D and 2D plots showed that pioglitazone binds through 2 conventional H-bond interactions with LYS364, ARG262; one Carbon H-bond interaction with GLU406; one Pi-Cation interaction with ARG262, one Pi-Anion interaction with GLU406; one Pi-Alkyl interaction with ARG262; two Alkyl interaction with ARG262, LYS258. The Chimera and Vina score result shows its potential energy of interaction is -6.4 kcal/mol (Table 13).

The molecular docking of vindoline (CID: 425978) with PPARγ (Figure 10) has shown its minimum binding affinity conformer, and non-covalent interactions and established that vindoline firmly binds to the around catalytic site ASN403, chain B of the PPARγ through 3 conventional H-bond interaction with ARG262; one Carbon H-bond interaction with GLU406 (Table 13). The best conformer minimal potential energy of molecular docked pose at a selected coordinate of vindoline and PPARγ target protein is -6.1 kcal/mol whereas PPARγ-Pioglitazone is -6.4 kcal/mol.

Table 13: Molecular docking analysis: Binding energy and the type of molecular interaction of control drugs and active compound of *C. roseus* against PPARγ.

Compounds	Vina Score/Binding Affinity (kcal/mol)	Ligand	Distance(Å)	Target Protein	Category	Type of Interaction
PPARy - Pioglitazone (Control)	-6.4	UNL1:O	2.18	B:LYS364:HN	Hydrogen Bond	Conventional H-Bond Interaction
		UNL1:O	2.82	B:ARG262:HH12	Hydrogen Bond	Conventional H-Bond Interaction
		UNL1:C	3.29	B:GLU406:OE1	Hydrogen Bond	Carbon H-bond interaction
		UNL1	3.92	B:ARG262:NH2	Non-Covalent Molecular Interaction	Pi-Cation Interaction
		UNL1	4.95	B:GLU406:OE1	Non-Covalent Molecular Interaction	Pi-Anion Interaction
		UNL1	5.49	B:ARG262	Hydrophobic	Pi-Alkyl Interaction
		UNL1:C	4.21	B:ARG262	Hydrophobic	Alkyl Interaction
		UNL1:C	4.09	B:LYS258	Hydrophobic	Alkyl Interaction
PPARy-Vindoline (Test)	-6.1	UNL1:O	2.51	B:ARG262:HH11	Hydrogen Bond	Conventional H-Bond Interaction
		UNL1:O	2.07	B:ARG262:HH11	Hydrogen Bond	Conventional H-Bond Interaction
		UNL1:O	2.02	B:ARG262:HH12	Hydrogen Bond	Conventional H-Bond Interaction
		UNL1:O	2.87	B:GLU406:HA	Hydrogen Bond	Carbon H-bond Interaction

Abbreviations: UNL: *C. roseus* active compounds, LYS: Lysine, ARG: Arginine, GLU: Glutamic acid.

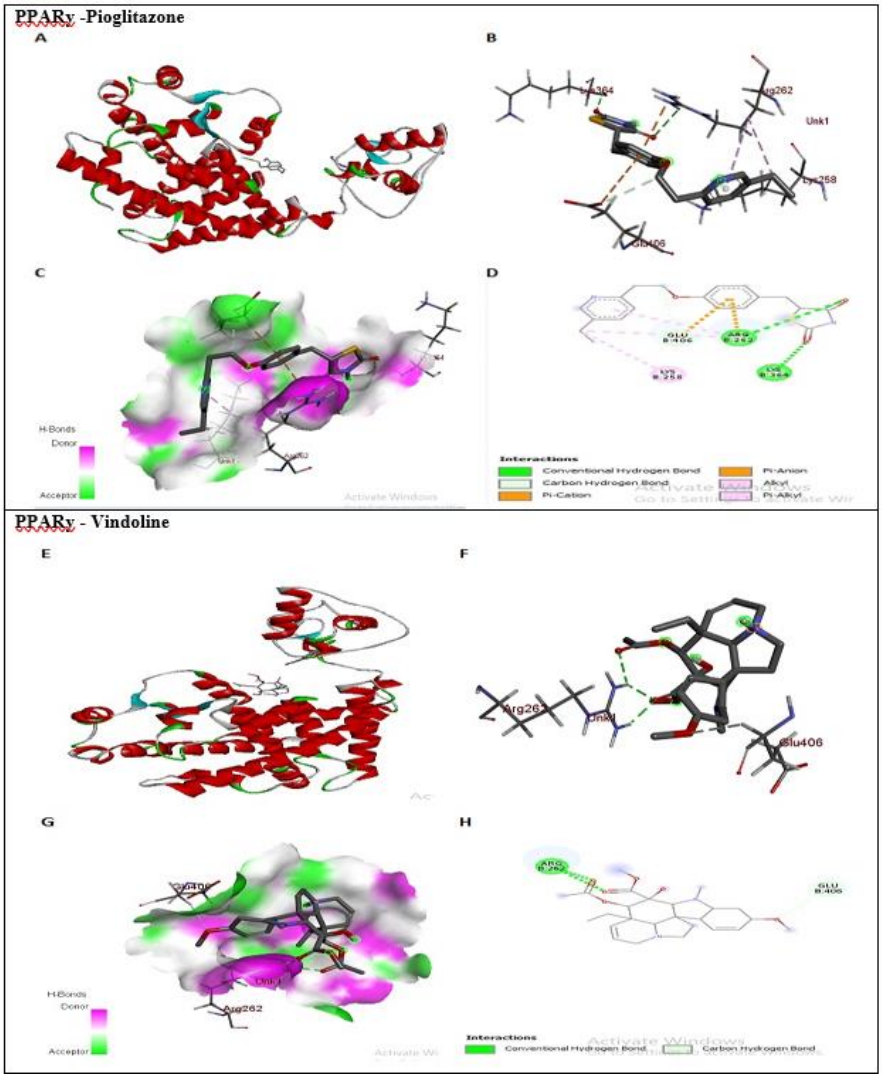

Figure 10: Molecular docking pose of PPARy and Control ligand (Pioglitazone) and test ligand (Vindoline). **(A)** Shows interaction between PPARy and agonist pioglitazone, **(B)** Related to target residues interaction with control ligand, **(C)** 3-D image of interactions on the target H-surface and pioglitazone, **(D)** 2-D diagram representing interactions between PPARy target and the control drug. Similarly, **(E)** Molecular docking pose view of vindoline with PPARy in its catalytic active site, **(F)** Signifies interaction between amino acids residue of the target and test compound vindoline, **(G)** Three-dimensional picture showing hydrogen bond donor and acceptor characteristics of the target surface and interaction of vindoline ligand with it, **(H)** 2-D diagram of interactions between PPARy and vindoline.

The deformability graph (Figure 11A) of the docked complexes shows the 9 hinges corresponding to deformable regions in the PPARγ proteins, with the greatest peak (1) Representing high deformability regions, 2 between 0.8 -1, 6 between 0.4-0.6. The B-factors mobility (Figure 11B) graph shows the strong correlation between experimental PDB and Simulation NMA results. The eigenvalue of PPARγ and vindoline complex is 4.56e-06 (Figure 11C). Variance (Figure 11D) Covariance, (Figure 11E) and Elastic networks plot (Figure 11F) show less stiffness of protein, presence of positive correlation and flexible binding between ligand vindoline and PPARγ docked complex respectively.

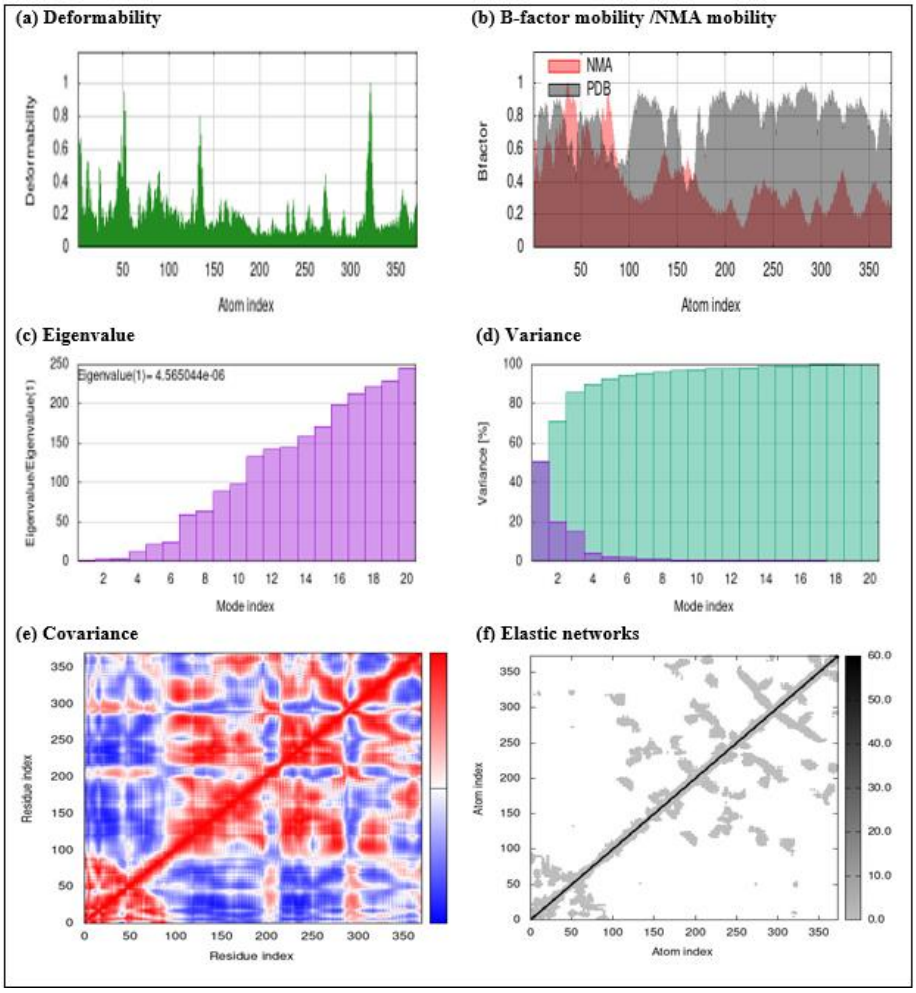

Figure 11: MD simulations results of docked complex PPARy-vindoline (ID:0706171335705).

Moreover, Pioglitazone (-6.4 kcal/mol) can bind tightly with PPARγ and stimulate the nuclear receptor, and a similar interaction is detected in vindoline (-6.1 kcal/mol) too. Thus, the alkaloid has good affinity with receptors and may control the PPARγ activity. The computational result shows that the biomolecules may become a PPARγ agonist drug and are effective as a 4th line of antidiabetic drug (patients having cardiac problems) too [55,56].

DISCUSSION

Since diabetes promotes multifactorial disease conditions in chronic cases. In this research, we observed that a natural compound vindoline (CID: 425978) acts as a more potent stimulator of AMPK than 1st line drug metformin. The binding affinity of vindoline alkaloids with AMPK1 and AMPK2 are -6.3 kcal/mol and -6.2 kcal/mol whereas metformin is -4.0 kcal/mol and -4.2 kcal/mol respectively. The eigenvalue of MD simulation for a docked complex of vindoline with targets AMPK1 (3.69e-06), and AMPK2 (5.18e-06) supports stable, flexible and strong interaction between them. The lower binding free energy of vindoline may be due to the formation of more stable noncovalent interactions (like H-bond, carbon H-bond interactions etc.). Similarly, the interaction between vindoline and α/β-tubulin (PDB 1Z2B) (docking result -7.28 kcal/mol) showed that vindoline enhances the defence mechanism in plants and has an inhibitory effect on cancer cells [57].

The research highlights that vindoline is a more potent stimulator of AMPK than metformin. Activated AMPK2 by phosphorylating IRS1, PFKFB2 and PFKFB3 components governs insulin-signalling and glycolysis pathway

and by phosphorylating CRTC2/TORC2 controls glucose homeostasis in the liver [10]. So, the AMPK2 stimulator can promote the phosphorylation activity of metabolic enzymes and decrease intracellular ATP levels inhibit mitochondrial complex I of the electron transport chain encourage peripheral glucose consumption through anaerobic glycolysis [8], increase GLP-1 plasma levels, stimulate peroxisome proliferator-activated receptor (PPARγ) mechanism and overcome Insulin resistance. As a result, it decreases hepatic glucose production, promotes the intake of glucose in skeletal muscle, and reduces blood glucose levels [10-13]. As a result, it affects the biosynthesis of protein, carbohydrates and lipids and inhibits cell growth and proliferation [10].

Target DPP4 is involved in the degradation of incretin and promotes blood glucose levels. Docking results show that the binding affinity of vindoline (CID: 425978) -6.8 kcal/mol is greater than the DPP4 inhibitor, vildagliptin (-6.7 kcal/mol). MD simulation eigenvalue 1.12e-04 of docked complex DPP4-vindoline supports that the complexes have good interaction, stability and molecular mobility. So, it may become a potent DPP-4 inhibitor and may become a good 2nd line therapeutic alternative for the treatment of diabetes. It is reported that the MERS-CoV virus binds with DPP4 and penetrates inside the cell [58] and vindoline binds strongly with beta-corona virus polymerase (docking energy score -6.8 kcal/mol) by interacting with its catalytic residues ASP644 and inhibits the enzymatic activity, replication and multiplication of virus [59].

Our research supports that vindoline acts as a potent inhibitor of the Dipeptidyl Peptidase-4 (DPP4) enzyme. Thus, binds competitively and selectively to the target site and inhibits degradation of incretin GLP-1 and GIP [15] and an increase in the level of them indirectly influences insulin secretagogues stimulates postprandial insulin discharge, and reduces glucagon secretion. As a result, it lowers fasting blood glucose levels in type 2 diabetics [16]. At the same time also support that inhibiting DPP4 reduces coronavirus infection and related seriousness in diabetic patient too.

Target α-glucosidase promotes glucose absorption in the intestine and increases blood glucose levels. Current research shows that the binding affinity of acarbose (-6.7 kcal/mol) is lower than the binding affinity of vindoline (CID: 425978) -6.8 kcal/mol. MD simulation supports structural dynamics of docked complex alpha glucosidase-vindoline (eigenvalue 1.96e-04) and has high-quality interaction, firmness and molecular mobility. The outcome of the study supports that vindoline has a strong α-glucosidase inhibition ability and become a potent 3rd line drug for diabetes. So, it has a better capability to decrease and regulate the plasma glucose concentration after a meal. Similarly, substituted aryl aldehyde inhibits α-glucosidase by binding to its C-terminal (IC50 values = 5.31 to 53.34 μM) [60]. As per our research finding α-glucosidase inhibitor vindoline can inhibit oligosaccharide binding to α-glucosidase enzyme and or delay their cleavage into monosaccharides from the active site of the α-glucosidase enzyme [6,14]. So, it slows down monosaccharide formation and its absorption and as a result checks the increase in postprandial glucose level.

As per the *in-silico* docking score of agonist Pioglitazone with PPARγ is -6.4 kcal/mol and vindoline is -6.1 kcal/mol. MD simulation of PPARγ-vindoline docked complex (eigenvalue 34.56e-06) supports stability, molecular mobility and the structural dynamics of the docked complexes. This shows that the vindoline alkaloids have good affinity with nuclear receptors and efficiently stimulate PPARγ activity. Moreover, PPARγ agonist acts as a 4th line drug and good therapeutic effect in diabetes-induced cardiac problem cases. Docking studies result (-

5.75 kcal/mol) of Quadrangularin A of Cissus quadrangularis Linn with PPARγ showed that it has a crucial role in the management of chronic cases of diabetes [61]. Hence, the binding of vindoline with PPARγ followed by activated PPARγ binds with PPAR response elements (PPRE) of DNA and controls the transcription of genes of glucose and lipids metabolism (e.g. acyl-CoA oxidase). Signals generated from the adipose tissue, e.g. adiponectin or leptin, may mediate the improvement in skeletal glucose disposal [20]. Also, PPARγ agonist promotes insulin sensitivity and insulin-stimulated glucose acceptance in peripheral tissues (hepatic, muscle, and adipose tissue) and differentiation of pre-adipocytes [19,55]. As a result, it may be able to control glucose homeostasis, the beta-oxidation pathway of fatty acids of peroxisome and regulate adipocyte differentiation [10].

Cell line (pancreatic β-TC6 or myoblast C2C12 cells) study of vindoline, vindolidine, vindolicine and vindolinine alkaloids reported that the alkaloid inhibits protein tyrosine phosphatase-1B (PTP-1B) activity and stimulate insulin sensitizer and antioxidant potential [32]. Also, in vitro study in Wistar rats, the antihyperglycemic effect of vindoline was tested and the result confirmed that vindoline decreases fasting blood glucose level (FBG) ($p < 0.05$) and hyperglycemia-induced hepatic injury and enhances the in vitro insulin secretion and improves both the hepatic and pancreatic tissues [62]. Also, in diabetes-induced kidney disorder, the structure of the renal parenchyma is improved and significantly reduced caspase 9 expression, and lipid peroxidation [63]. It reduces glucose-induced toxicity and intracellular reactive oxygen species generation in cells [64].

Many researchers reported that *C. roseus* has a hypoglycemic effect better than existing alpha-glucosidase inhibitors and biguanides and also nullifies the possibility of diarrhoea-related toxicity [13]. Its therapy works on blood glucose homeostasis, protein, and lipid metabolisms, stimulating glycogen synthesis and boosting glucose utilization in the liver [31]. A lot of research reported that ethanolic extract of *Catharanthus roseus* significantly reduces the high glucose level as well as improves antioxidant defence systems ($P \leq 0.05$) in both serum and RBC in addition to histopathological studies supporting that its ability to heal pancreas beta-cells with its regeneration possibilities [64]. Literature also supported its positive effect on other enzymes such as succinate dehydrogenase, glycogen synthase, glucose-6-phosphate-dehydrogenase and malate dehydrogenase [30].

Our prediction model studies supported with previous experimental validation outcome provides high possibilities for the use of putative drug candidate vindoline (CID: 425978) biomolecule as a potent multi-targeted antidiabetic drug. The outcome will further be validated by wet lab tests and clinical trials for drug design and discovery.

CONCLUSION

Present studies, provide evidence for 3D confirmation of vindoline having PubChem CID: 425978 has the potential to act on multiple targets of glucose regulation pathway and show stable, flexible binding and more efficient binding energy potential than existing standard antidiabetic drugs. Also, vindoline has antiviral properties and can inhibit the binding and replication of the human coronavirus. Based on the outcome, we can say that the biomolecules can become a potent antidiabetic drug that can control blood glucose levels as well as its secondary complications. Furthermore, it addresses the futuristic vital pharmacological issues of diabetes mellitus and will open multiple therapeutic drug target disease-related research possibilities, which will be confirmed by future studies.

ETHICAL STATEMENTS

The current research article work was performed by computational tools, without using any scientific lab animals, human samples or any human patients. Thus, no official permission was taken from our research team against the research article from the ethical committee of our university and government.

ACKNOWLEDGMENT

Richa Goyal is thankful to Dr. Ashish Kumar Biswas (HOD and Associate Professor, Pharmacology Department, Sheikh Bhikhari Medical College and Hospital Hazaribagh,Jharkhand, India); Dr. Mukesh Nitin (Head of Department of Tech. Data Sci. & Biosciences, Digianalix, Ranchi, Jharkhand, India) for guidance and feedback; Research scientific officer Priyangulta Beck, Account officer Vinita Kumari and Student Dipanjali Sharma (Department of Tech. Data Sci. & Biosciences, Digianalix, Ranchi, Jharkhand, India) for their support.

FUNDING

The authors have received no external financial support for the research and publication of this article.

CONFLICTING INTEREST

All the authors declared that there is no conflict of interest associated with any of the senior authors or other contributors in this manuscript.

REFERENCES

1. Kasper DL, Fauci AS, Longo, DL et al. (2005) Harrison's principles of internal medicine. 16th (Edn.), Mc Graw Hill Publication, USA.
2. Saeedi P, Petersohn I, Salpea P et al. (2019) Global and regional diabetes prevalence estimates for 2019 and projections for 2030 and 2045: Results from the International Diabetes Federation Diabetes Atlas. Diabetes Research and Clinical Practice 157: 107843.
3. Singh U (2016) Prevalence of diabetes and other health related problems across India and worldwide: An overview. Journal of Applied and Natural Science 8(1): 500-505.
4. Proença C, Ribeiro D, Freitas M et al. (2022) Flavonoids as potential agents in the management of type 2 diabetes through the modulation of α-amylase and α-glucosidase activity: A review. Critical Reviews in Food Science and Nutrition 62(12): 3137-3207.
5. Kashtoh H and Baek KH (2022) Recent updates on phytoconstituent alpha-glucosidase inhibitors: An approach towards the treatment of type two diabetes. Plants 11(20): 2722.
6. Lebovitz HE (1997) Alpha-glucosidase inhibitors. Endocrinology and Metabolism Clinics of North America 26(3): 539-551.
7. Hall JE and Guyton AC (2011) Guyton and hall textbook of medical physiology. 12th (Edn.), Saunders Elsevier publication.
8. Tripathi KD (2010) Essentials of medical pharmacology. 6th (Edn.), JAYPEE publication.
9. Alam S, Sarker MMR, Sultana TN, et al. (2022) Antidiabetic phytochemicals from medicinal plants: Prospective candidates for new drug discovery and development. Frontiers in Endocrinology 13: 800714.

10. The uniProt consortium (2021) UniProt: The universal protein knowledgebase in 2021. Nucleic Acids Research 49: D480-D489.
11. Foretz M, Guigas B, Bertrand L, et al. (2014) Metformin: From mechanisms of action to therapies. Cell Metabolism 20(6): 953-966.
12. Foretz M, Guigas B, Viollet B (2019) Understanding the glucoregulatory mechanisms of metformin in type 2 diabetes mellitus. Nature Reviews Endocrinology 15(10): 569-589.
13. Ohadoma SC, Akpan JL, Odey PA et al. (2021) Mechanistic considerations of *Catharanthus roseus* on the hypo-glycemic activity of alpha glucosidase inhibitors and biguanides: A review. Journal Of Pharmaceutical Advanced Research 4: 1390-1398.
14. Prabhakar P and Banerjee M (2020) Antidiabetic phytochemicals: A comprehensive review on opportunities and challenges in targeted therapy for herbal drug development. International Journal of Pharmaceutical Research 1: 1673-1696.
15. Ahrén B, Schweizer A, Dejager S, et al. (2011) Mechanisms of action of the dipeptidyl peptidase-4 inhibitor vildagliptin in humans. Diabetes, Obesity and Metabolism 13(9): 775-783.
16. Baptist G (2019) Clinical use of DPP-4 inhibitors. Frontiers in Endocrinology 10,389: 1-10.
17. Jiang J and Ghosh S (2019) Alpha glucosidase - diabetes mellitus: Drugs - PDB-101: 6b00992.
18. Derosa G and Maffioli P (2012) α-Glucosidase inhibitors and their use in clinical practice. Archives of Medical Science: AMS 8(5): 899-906.
19. Chandra A, Kaur P, Sahu SK et al. (2022) A new insight into the treatment of diabetes by means of pan PPAR agonists. Chemical Biology & Drug Design 100(6): 947-967.
20. Bailey CJ and Day C (2001) Thiazolidinediones today. The British Journal of Diabetes & Vascular Disease 1(1): 7-13.
21. Adhikari B (2021) Roles of alkaloids from medicinal plants in the management of diabetes mellitus. Journal of Chemistry 2021: 1-10.
22. Kalhotra P, Chittepu VC, Osorio-Revilla G et al. (2020) Phytochemicals in garlic extract inhibit therapeutic enzyme DPP-4 and induce skeletal muscle cell proliferation: A possible mechanism of action to benefit the treatment of diabetes mellitus. Biomolecules 10(2): 305.
23. Bharadwaj S, Dubey A, Yadava U, et al. (2021) Exploration of natural compounds with anti-SARS-CoV-2 activity via inhibition of SARS-CoV-2 M^{pro}. Briefings in Bioinformatics 22(2): 1361-1377.
24. Newman DJ and Cragg GM (2007) Natural products as sources of new drugs over the last 25 years. Journal of Natural Products 70(3): 461-477.
25. Bennouna J, Delord JP, Campone M et al. (2008) Vinflunine: A new microtubule inhibitor agent. Clinical Cancer Research 14(6): 1625-1632.
26. Mohan SC, Anand T, Priyadharshini GS et al. (2015) GC-MS analysis of phytochemicals and hypoglycemic effect of *Catharanthus roseus* in alloxan-induced diabetic rats. International Journal of Pharmaceutical Sciences Review and Research 31(1): 123-128.
27. Nisar A, Mamat AS, Hatim MI, et al. (2016) An updated review on *Catharanthus roseus*: Phytochemical and pharmacological analysis. Indian Research Journal of Pharmacy and Science 3(2): 631-653.
28. Tolambiya P and Mathur S (2016) A study on potential phytopharmaceuticals assets in *Catharanthus roseus L. (Alba)*. International Journal of Life Sciences Biotechnology and Pharma Research 5(1): 1-6.

29. John J (2017) Evaluation of hypoglycemic effect of Aloe vera on allaxon induced diabetic rats. International Journal of Information Research and Review 4(3): 3865-3868.
30. Mishra JN and Verma NK (2017) A brief study on *Catharanthus roseus*: A review. International Journal of Research in Pharmaceutical Sciences 2(2): 20-23.
31. Balaji DH (2014) Versatile. Therapeutic effects of *Vinca rosea Linn*. International Journal of Pharmaceutical Science and Health Care 1(4): 59-76.
32. Tiong SH, Looi CY, Hazni H, et al. (2013) Antidiabetic and antioxidant properties of alkaloids from *Catharanthus roseus (L.) G. Don*. Molecules 18(8): 9770-9784.
33. Elhassaneen Y, Ragab S, Abd El-Rahman A et al. (2021) Vinca (*Catharanthus roseus*) extracts attenuate alloxan-induced hyperglycemia and oxidative stress in rats. American Journal of Food Science and Technology 9(4): 161-172.
34. Srivastava V, Yadav A and Sarkar P (2022) Molecular docking and ADMET study of bioactive compounds of Glycyrrhiza glabra against main protease of SARS-CoV2. Materials Today: Proceedings 49: 2999-3007.
35. Bhattacharya R, Rose PW, Burley SK et al. (2017) Impact of genetic variation on three dimensional structure and function of proteins. PloS One 12(3): e0171355.
36. Schwede T, Kopp J, Guex N et al. (2003) SWISS-MODEL: An automated protein homology-modeling server. Nucleic Acids Research 31(13): 3381-3385.
37. Gasteiger E, Hoogland C, Gattiker A et al. (2005) Protein identification and analysis tools on the ExPASy server. Humana Press 571-607.
38. Geourjon C and Deleage G (1995) SOPMA: Significant improvements in protein secondary structure prediction by consensus prediction from multiple alignments. Bioinformatics 11(6): 681-684.
39. Hirokawa T, Boon-Chieng S and Mitaku S (1998) SOSUI: Classification and secondary structure prediction system for membrane proteins. Bioinformatics 14(4): 378-379.
40. Hollingsworth SA and Karplus PA (2010) A fresh look at the Ramachandran plot and the occurrence of standard structures in proteins. Biomolecular Concepts 1(3-4): 271-283.
41. Binkowski TA, Naghibzadeh S, Liang J (2003) CASTp: Computed atlas of surface topography of proteins. Nucleic Acids Research 31(13): 3352-3355.
42. Guex N and Peitsch MC (1997) SWISS-MODEL and the Swiss-Pdb Viewer: An environment for comparative protein modeling. Electrophoresis 18(15): 2714-2723.
43. Pettersen EF, Goddard TD, Huang CC et al. (2004) UCSF Chimera-a visualization system for exploratory research and analysis. Journal of Computational Chemistry 25(13): 1605-1612.
44. Eberhardt J, Santos-Martins D, Tillack AF et al. (2021) AutoDock Vina 1.2. 0: New docking methods, expanded force field, and python bindings. Journal of Chemical Information and Modeling 61(8): 3891-3898.
45. Kim S, Chen J, Cheng T, et al. (2021) PubChem in 2021: New data content and improved web interfaces. Nucleic Acids Research 49(D1): D1388-D1395.
46. O'Boyle NM, Banck M, James CA et al. (2011) Open babel: An open chemical toolbox. Journal of Cheminformatics 3(1): 1-14.
47. Sander T (2001) OSIRIS property explorer. Organic Chemistry Portal.
48. Bickerton GR, Paolini GV, Besnard J et al. (2012) Quantifying the chemical beauty of drugs. Nature Chemistry 4(2): 90-98.

49. Hanwell MD, Curtis DE, Lonie DC et al. (2012) Avogadro: An advanced semantic chemical editor, visualization, and analysis platform. Journal of Cheminformatics 4(1): 1-17.
50. Biovia DS (2015) Discovery studio modeling environment, Dassault Systèmes Release, San Diego, 4.
51. López-Blanco JR, Aliaga JI, Quintana-Ortí ES et al. (2014) iMODS: Internal coordinates normal mode analysis server. Nucleic Acids Research 42(W1): W271-W276.
52. Hamarsha A, Balachandran K, Sailan AT et al. (2023) Predicting Key Genes and Therapeutic Molecular Modelling to Explain the Association between *Porphyromonas gingivalis (P. gingivalis)* and Alzheimer's Disease (AD). International Journal of Molecular Sciences 24(6): 5432.
53. Rena G, Pearson ER, Sakamoto K (2013) Molecular mechanism of action of metformin: old or new insights?. Diabetologia 56: 1898-1906.
54. Zhou G, Myers R, Li Y et al. (2001) Role of AMP-activated protein kinase in mechanism of metformin action. The Journal of Clinical Investigation 108(8): 1167-1174.
55. Kahn CR, Chen L, Cohen SE (2000) Unraveling the mechanism of action of thiazolidinediones. The Journal of Clinical Investigation 106(11): 1305-1307.
56. Subramaniam S (1999) The emerging role of thiazolidinediones in the treatment of diabetes-mellitus and related disorders. Clinical and Experimental Hypertension 21(1-2): 121-136.
57. Sertel S, Fu Y, Zu Y et al. (2011) Molecular docking and pharmacogenomics of vinca alkaloids and their monomeric precursors, vindoline and catharanthine. Biochemical Pharmacology 81(6): 723-735.
58. Wang N, Shi X, Jiang L et al. (2013) Structure of MERS-CoV spike receptor-binding domain complexed with human receptor DPP4. Cell Research 23(8): 986-993.
59. Venkateshan M, Muthu M, Suresh J et al. (2020) Azafluorene derivatives as inhibitors of SARS CoV-2 RdRp: Synthesis, physicochemical, quantum chemical, modeling and molecular docking analysis. Journal of Molecular Structure 1220: 128741.
60. Taha M, Ismail NH, Lalani S et al. (2015) Synthesis of novel inhibitors of α-glucosidase based on the benzothiazole skeleton containing benzohydrazide moiety and their molecular docking studies. European Journal of Medicinal Chemistry 92: 387-400.
61. Patil VS, Biradar PR, Attar V et al. (2019) In silico docking analysis of active biomolecules from *Cissus quadrangularis L.* against PPAR-γ. Indian Journal of Pharmaceutical Education and Research 53(3): S332-S337.
62. Goboza M, Aboua YG, Chegou N et al. (2019) Vindoline effectively ameliorated diabetes-induced hepatotoxicity by docking oxidative stress, inflammation and hypertriglyceridemia in type 2 diabetes-induced male Wistar rats. Biomedicine & Pharmacotherapy 112: 108638.
63. Oguntibeju OO, Aboua Y, Goboza M (2019) Vindoline-a natural product from *Catharanthus roseus* reduces hyperlipidemia and renal pathophysiology in experimental type 2 diabetes. Biomedicines 7(3): 59.
64. Goboza M, Meyer M, Aboua YG et al. (2020) In vitro antidiabetic and antioxidant effects of different extracts of *Catharanthus roseus* and its indole alkaloid, vindoline. Molecules 25(23): 5546.